

INVESTIGATION INTO THE PATHOGENESIS OF RETINAL
DYSPLASIA IN THE MINIATURE SCHNAUZER AND ENGLISH
SPRINGER SPANIEL DOG

A Thesis Submitted to the College of
Graduate Studies and Research
in Partial Fulfillment of the Requirements
for the Degree of Masters of Science
in the Department of Small Animal Clinical Sciences
Western College of Veterinary Medicine
University of Saskatchewan
Saskatoon

By

Bianca Susanne Bauer

© Copyright Bianca Susanne Bauer, December 2008. All rights reserved.

PERMISSION TO USE

In presenting this thesis/dissertation in partial fulfillment of the requirements for a Postgraduate degree from the University of Saskatchewan, I agree that the Libraries of this University may make it freely available for inspection. I further agree that permission for copying of this thesis/dissertation in any manner, in whole or in part, for scholarly purposes may be granted by the professor or professors who supervised my thesis/dissertation work or, in their absence, by the Head of the Department or the Dean of the College in which my thesis work was done. It is understood that any copying or publication or use of this thesis/dissertation or parts thereof for financial gain shall not be allowed without my written permission. It is also understood that due recognition shall be given to me and to the University of Saskatchewan in any scholarly use which may be made of any material in my thesis/dissertation.

DISCLAIMER

Reference in this thesis/dissertation to any specific commercial products, process, or service by trade name, trademark, manufacturer, or otherwise, does not constitute or imply its endorsement, recommendation, or favoring by the University of Saskatchewan. The views and opinions of the author expressed herein do not state or reflect those of the University of Saskatchewan, and shall not be used for advertising or product endorsement purposes.

Requests for permission to copy or to make other uses of materials in this thesis/dissertation in whole or part should be addressed to:

Head of the Department of Small Animal Clinical Sciences
Western College of Veterinary Medicine
University of Saskatchewan
Saskatoon, Saskatchewan
S7N 5B4
Canada

OR

Dean
College of Graduate Studies and Research
University of Saskatchewan
107 Administration Place
Saskatoon, Saskatchewan
S7N 5A2
Canada

ABSTRACT

INVESTIGATION INTO THE PATHOGENESIS OF RETINAL DYSPLASIA IN THE MINIATURE SCHNAUZER AND ENGLISH SPRINGER SPANIEL DOG

Bianca S. Bauer, BSc., DVM
University of Saskatchewan, 2008
DipACVO

Supervisor:
Lynne S. Sandmeyer, DVM,

Retinal dysplasia has been documented in many breeds of dogs. It has recently been hypothesized that Miniature Schnauzer dogs affected with retinal dysplasia and associated persistent hyperplastic primary vitreous have a decreased amount of *Tfam* and several mtDNA transcripts in the retina and RPE. Affected dogs were also hypothesized to have a decrease in leukocyte mtDNA compared to normal dogs. Additionally, using electron microscopy, these dogs were hypothesized to having decreased mitochondrial numbers and size with altered morphology in multiple tissues, including neutrophils. Due to these recent discoveries in this breed it has been proposed that retinal dysplasia could be the result of an altered energy supply to the retina and RPE. The objective of this study was to further investigate the pathogenesis of retinal dysplasia in the Miniature Schnauzer and English Springer Spaniel dog.

The hypothesis of an altered *Tfam* gene sequence in affected Miniature Schnauzer dogs leading to a decreased amount of *Tfam* transcript in the retina and RPE was tested by amplifying, cloning and sequencing the coding, 5' and 3' non-coding regions, and intron 1 of the *Tfam* gene from affected and normal Miniature Schnauzer dogs. Using transmission electron microscopy, affected and normal lymphocyte mitochondria were also objectively measured and quantified in this breed along with mitochondrial morphology assessment. In the English Springer Spaniel dog, the hypothesis of a decreased amount of leukocyte mtDNA in affected dogs was tested using real-time PCR. In addition, using transmission electron microscopy, affected and normal lymphocyte mitochondria were objectively measured and quantified in this breed with mitochondrial morphology assessment.

Sequencing of the particular regions of the Miniature Schnauzer *Tfam* gene revealed no significant nucleotide changes between affected and normal dogs. Evaluation of lymphocyte mitochondrial size, number and morphology also revealed no significant

differences between the two groups. In the English Springer Spaniel dog a relative decrease in leukocyte mtDNA did not exist in dogs affected with retinal dysplasia. Furthermore, evaluation of affected English Springer Spaniel dog lymphocyte mitochondria revealed no significant differences in mitochondrial number, surface area or morphology when compared to normal English Springer Spaniel dogs.

To conclude, we failed to demonstrate a mutation in the areas of the *Tfam* gene sequenced in Miniature Schnauzers affected with retinal dysplasia and associated persistent hyperplastic primary vitreous. In contrast to previous findings of decreased leukocyte mtDNA in the affected Miniature Schnauzer dog, no evidence was found to support a relative decrease in leukocyte mtDNA in English Springer Spaniel dogs affected with retinal dysplasia. Furthermore, the hypothesis of altered mitochondrial size, number and morphology in affected dogs is not supported by this study. Further evaluation of mitochondria, mtDNA and mitochondrial gene expression within age-matched retina and RPE of Miniature Schnauzer and English Springer Spaniel dogs is necessary to determine if mitochondria and altered energy supply play a role in the pathogenesis of retinal dysplasia in these breeds.

ACKNOWLEDGEMENTS

I would not have been able to complete this project without the aid and support of countless people over the past two years. I would like to first express my gratitude towards Drs. Lynne Sandmeyer and Bruce Grahm. Their leadership, support, attention to detail and hard work have set an example I hope to match some day. I would like also like to express my gratitude to Dr. George Forsyth, whose expertise, understanding, and patience added considerably to my graduate experience. A special thanks also goes out to the other members of my committee, Drs. Janet Hill and Klaas Post, for the assistance they provided at all levels of the research project. Appreciation also goes out to Darlene Hall, Jennifer Cowell and Ian Shirley for all of their technical assistance throughout my graduate program. I must also thank Cathy McMillan for her dedication to our research. The Miniature Schnauzers are truly fortunate to have you, Cathy.

I thank my grandmother, Maria Magdalena. Although this journey has taken me further away from her in distance, it has only brought me closer to her emotionally. Her love and confidence in me has helped me in countless ways. I also thank my sisters for being with me from the very beginning. You are my best friends and I am thankful for your support. Most importantly, I thank my mother for instilling in me the confidence and determination to pursue a Masters of Science. It is not possible to summarize the magnitude of the influence my mother has had on me. She is a true role model of strength and determination and her unconditional support and encouragement every step of the way means more to me than she will ever know. Lastly, many thanks to the rest of my family and friends who helped me get through graduate school. Even though they are 3000 km away they have been a great source of strength throughout this work.

In conclusion, I recognize that this research would not have been possible without the financial assistance of the Companion Animal Health Fund and I express my gratitude to this agency.

DECLARATION OF WORK PERFORMED

I, Bianca Susanne Bauer, declare that this thesis is my own original work, conducted under the supervision of Dr. Lynne Sandmeyer. It is submitted for the degree of a Master of Science at the University of Saskatchewan. The work performed for this thesis was carried out in the Veterinary Biomedical Science department at the Western College of Veterinary Medicine, University of Saskatchewan between July 2006 and July 2008. All experimental results were obtained by me alone and to the best of my knowledge have not been published previously by any other person. No part of this research has been submitted in the past, or is being submitted, for a degree or examination at any other university.

TABLE OF CONTENTS

PERMISSION TO USE	i
ABSTRACT.....	iii
ACKNOWLEDGMENTS.....	v
DECLARATION OF WORK PERFORMED.....	vi
TABLE OF CONTENTS.....	vii
LIST OF TABLES.....	ix
LIST OF FIGURES.....	x
LIST OF EQUATIONS.....	xii
LIST OF ABBREVIATIONS.....	xiii

GENERAL INTRODUCTION

Retinal Dysplasia in Dogs	1
Histopathology	3
Etiology	4
Pathogenesis.....	5
Recent Discoveries in Retinal Dysplasia.....	6
Study Objectives	7

GENERAL LITERATURE REVIEW

Section 1

Regulation of Nuclear Gene Expression.....	13
Nuclear Gene Transcription and Polyadenylation.....	13
Mitochondrial Genetics.....	14
Mitochondrial Transcription and Transcription Factor A (TFAM)	16
The Polymerase Chain Reaction (PCR)	17

Section 2

Retinal Dysplasia in the English Springer Spaniel Dog.....	20
Real-time Polymerase Chain Reaction.....	21

CHAPTER 1

NUCLEOTIDE SEQUENCING FOR THE MITOCHONDRIAL TRANSCRIPTION FACTOR A GENE (*Tfam*) AND LYMPHOCYTE MITOCHONDRIAL QUANTIFICATION AND MEASUREMENT IN MINIATURE SCHNAUZER DOGS AFFECTED WITH INHERITED RETINAL DYSPLASIA AND ASSOCIATED PERSISTENT HYPERPLASTIC PRIMARY VITREOUS

1.1 Introduction.....	29
1.2 Materials and Methods.....	31
1.3 Results.....	35
1.4 Discussion.....	37

CHAPTER 2

RELATIVE QUANTITATION OF LEUKOCYTE MITOCHONDRIAL DNA AND MITOCHONDRIAL EVALUATION USING TRANSMISSION ELECTRON MICROSCOPY IN NORMAL ENGLISH SPRINGER SPANIEL DOGS AND THOSE AFFECTED WITH RETINAL DYSPLASIA

2.1 Introduction.....	52
2.2 Materials and Methods.....	54
2.3 Results.....	58
2.4 Discussion.....	60

GENERAL CONCLUSION.....	76
--------------------------------	-----------

REFERENCES	79
-------------------------	-----------

LIST OF TABLES

CHAPTER 1

Table 1.1	<i>Tfam</i> oligonucleotide primer sequences.....	42
Table 1.2	Lymphocyte surface area and mitochondrial quantification and surface area measurement using electron microscopy of normal and affected Miniature Schnauzer dogs	43

CHAPTER 2

Table 2.1	Comparison of crossing threshold (CT) for COX-1 and GA-3-PDH for unaffected English Springer Spaniel dogs.....	64
Table 2.2	Comparison of crossing threshold (CT) for COX-1 and GA-3-PDH for affected English Springer Spaniel dogs.....	65
Table 2.3	Lymphocyte surface area and mitochondrial quantification and surface area using measurement using electron microscopy of normal and affected English Springer Spaniel dogs.....	66

LIST OF FIGURES

GENERAL INTRODUCTION

Figure 1	Multifocal retinal dysplasia.....	8
Figure 2	Geographic retinal dysplasia.....	9
Figure 3	Histologic section of retinal dysplasia.....	10
Figure 4	Transmission electron micrographs of normal and affected Miniature Schnauzer neutrophils.....	11
Figure 5	Transmission electron micrographs of normal and affected Miniature Schnauzer skeletal muscle	12

GENERAL LITERATURE REVIEW

Figure 1	Map of mammalian mtDNA.....	24
Figure 2	TFAM gene structure.....	25
Figure 3	Electron micrographs of control (<i>Tfam</i> ⁺ / <i>Tfam</i> ⁺) and homozygous Knockout embryo (<i>Tfam</i> ⁻ / <i>Tfam</i> ⁻) mitochondria.....	26
Figure 4	Real-time PCR amplification plots.....	27
Figure 5	Dissociation curve of a real-time amplicon.....	28

CHAPTER 1

Figure 1.1	TFAM gene structure.....	44
Figure 1.2	Transmission electron micrograph of a canine lymphocyte.....	45
Figure 1.3	Multiple alignment of <i>Tfam</i> promoter sequences from affected and normal Miniature Schnauzer dogs compared to GenBank [®] accession number NC_006586.....	46
Figure 1.4	Multiple alignment of <i>Tfam</i> intron1 sequences from affected and normal Miniature Schnauzer dogs compared to GenBank [®] accession number NC_006586.....	47
Figure 1.5	Multiple alignment of the <i>Tfam</i> 3' non-coding region from affected and normal Miniature Schnauzer dogs compared to GenBank [®] accession number NC_006586.....	48

Figure 1.6	Box and whisker graphs of lymphocyte surface area of normal and affected Miniature Schnauzer dogs.....	49
Figure 1.7	Box and whisker graphs of mitochondrial numbers per lymphocyte of normal and affected Miniature Schnauzer dogs.....	50
Figure 1.8	Box and whisker graphs of mitochondrial surface area of normal and affected Miniature Schnauzer dogs.....	51

CHAPTER 2

Figure 2.1	Transmission electron micrograph of a canine lymphocyte.....	67
Figure 2.2	Standard curve for GA-3-PDH.....	68
Figure 2.3	Standard curve for COX-1.....	69
Figure 2.4	Bar graphs depicting relative amount of leukocyte mtDNA from normal English Springer Spaniel dogs.....	70
Figure 2.5	Bar graphs depicting relative amount of leukocyte mtDNA from affected English Springer Spaniel dogs calibrated to a normal dog	71
Figure 2.6	Dissociation analysis of real-time COX-1 and GA-3-3PDH amplicons.....	72
Figure 2.7	Box and whisker graphs of lymphocyte surface area of normal and affected English Springer Spaniel dogs.....	73
Figure 2.8	Box and whisker graphs of mitochondrial numbers per lymphocyte cross-section of normal and affected English Springer Spaniel dogs	74
Figure 2.9	Box and whisker graphs of mitochondrial surface area per lymphocyte cross-section of normal and affected English Springer Spaniel dogs.....	75

LIST OF EQUATIONS

GENERAL LITERATURE REVIEW

Equation 1.	Calculation of the frequency of occurrence of a nucleotide sequence in a genome.....	18
Equation 2.	Calculation of the final copy number of amplified sequence after PCR.....	18
Equation 3.	Calculation of PCR efficiency in the exponential phase of the reaction.....	19
Equation 4.	Calculation of real-time PCR amplification efficiency using the slope of a standard curve.....	22
Equation 5.	Calculation of ΔC_T by normalization of C_T	22
Equation 6.	Calculation of $\Delta\Delta C_T$ by calibration of ΔC_T	22
Equation 7.	Calculation of the relative amount of a target to a calibrator using the $\Delta\Delta C_T$ method.....	23
Equation 8.	Calculation of the relative amount of a target to a calibrator using the Pfaffl method.....	23

LIST OF ABBREVIATIONS

A – adenosine
AS – antisense
ATP – adenosine-5'-triphosphate
bp – base pairs
C – cytosine
cDNA – complementary deoxyribonucleic acid
COX-1 – cytochrome oxidase subunit 1
 C_T – threshold cycle
dATP – deoxyadenosine triphosphate
dCTP – deoxycytidine triphosphate
dc⁷GTP – 7-deaza-2'-deoxyguanosine-5'triphosphate dilithium salt
dGTP – deoxyguanosine triphosphate
D-loop – displacement-loop
DNA – deoxyribonucleic acid
dNTP – deoxyribonucleoside triphosphate
dsDNA – double stranded deoxyribonucleic acid
dTTP – deoxythymidine triphosphate
G – guanine
GA-3-PDH – glyceraldehyde-3-phosphate-dehydrogenase
HMP – high mobility group
HSP – heavy strand promoter
LSP – light strand promoter
mRNA – messenger ribonucleic acid
mtDNA – mitochondrial deoxyribonucleic acid
NADH – the reduced form of nicotinamide adenine dinucleotide
NRF-1 – nuclear respiratory factor 1
NRF-2 – nuclear respiratory factor 2
PABP – poly(A) binding protein
PCR – polymerase chain reaction

PGC-1 α – peroxisome proliferator-activated receptor- γ coactivator-1 α

PHPV – persistent hyperplastic primary vitreous

PHTVL – persistent hyperplastic tunica vasculosa lentis

POLRMT – mitochondrial ribonucleic acid polymerase

PRC – PGC-1-related-coactivator

RDA – representational difference analysis

RNA – ribonucleic acid

rRNA - ribosomal ribonucleic acid

RPE – retinal pigment epithelium

S – sense

T – thymidine

TFAM – mitochondrial transcription factor A

TFB1M – mitochondrial transcription factor B1

TFB2M – mitochondrial transcription factor B2

T_m – melting temperature

tRNA - transfer ribonucleic acid

GENERAL INTRODUCTION

RETINAL DYSPLASIA IN DOGS

Retinal dysplasia is a common congenital disorder in dogs and is defined as an abnormal differentiation of the sensory layers of the retina.¹ The condition was first recognized in the Bedlington Terrier by Rubin in 1963^{2,3}, and has since been reported in many breeds.⁴⁻¹⁷ Morphologically, retinal dysplasia can be classified into three forms: i) single or multiple retinal folds; ii) geographic retinal dysplasia and iii) generalized dysplasia with retinal detachment or non-attachment.¹⁸ In focal or multiple retinal folds the lesions appear as grey or green linear streaks or dots and are most prevalent in the central tapetal fundus, dorsal to the optic disc. Dysplastic foci in the non-tapetal fundus appear as grey worm-like retinal opacities.^{9,19} (Figure 1) In geographic retinal dysplasia the affected areas appear irregular or have a horse-shoe shaped appearance.¹⁹ (Figure 2) Often within or around the dysplastic area retinal elevation may be noted, as well as hyperreflective areas indicative of neuroretinal degeneration.¹⁹ Lastly, in generalized retinal dysplasia with retinal detachment a completely detached neural retina is evident, often only attached at the optic nerve. In neonates, leukocoria and a rotary nystagmus may accompany generalized retinal dysplasia.¹⁹ The cause of retinal detachment in retinal dysplasia has not been determined. In the English Springer Spaniel dog it has been proposed that the presence of ectopic vessels within the dysplastic areas may compromise the inner blood-retinal barrier resulting in leakage and subsequent retinal detachment.²⁰ Vitreoretinal degeneration and liquefaction has been demonstrated to contribute to retinal detachment in Labrador retrievers²¹ and thus may also play a role in generalized retinal dysplasia in this breed.

Clinically, retinal dysplasia is non-progressive but lesions may change in appearance with age due to remodelling of the retina.^{4,19,20,22} In focal or multifocal retinal dysplasia the lesions occasionally become less obvious and some folds may disappear with time.¹⁹ In the geographic form the lesions often become more demarcated with time.¹⁹ The retinal pigment epithelium (RPE) underlying the dysplastic areas may appear more pigmented due to RPE hypertrophy or hyperplasia.¹⁹ Retinal dysplasia occurs both

bilaterally and unilaterally.¹⁸ Affected dogs may have normal or impaired functional vision or may present with unilateral or bilateral blindness due to retinal detachment or non-attachment.¹⁹

Although retinal dysplasia is believed to be congenital, Holle *et al.*²³ have proposed that a developmental form of geographic retinal dysplasia may also exist. This retrospective study identified geographic retinal lesions in various purebred and mixed breed dogs at 10 weeks of age. The lesions identified were not visualized in the same dogs between 5 and 9 weeks of age. The posterior pole and equatorial regions of the superior fundus were most commonly affected and lesions appeared as thick, dark, circular plaques of retinal tissue. The lesions were often accompanied by retinal folds and were usually associated with the major retinal vessels. The non-tapetal fundic lesions appeared as circular grey to white plaques and were located in the peripapillary region or along the horizontal retinal vascular arcades nasally or temporally. All lesions were unilateral and the authors proposed that the lesions identified were consistent with geographic retinal dysplasia.²³ This presumptive diagnosis may however, be erroneous. Retinal dysplasia is a defect of retinal differentiation and is thus considered to be a congenital condition.¹⁹ Lesions should therefore, be visible at birth and be predominately bilateral, however, all dogs examined in the study by Holle *et al.*²³ were normal before 10 weeks of age and all lesions were unilateral. Secondly, hereditary factors are suspected to be the cause of retinal dysplasia in most breeds.^{3, 4, 7, 9, 10, 13, 14, 24-26} Pedigree analysis or test breeding was not performed in this study to verify the diagnosis of an inherited condition. Most importantly, histopathology, which is necessary to confirm a diagnosis of retinal dysplasia, was not performed in this study. It is therefore likely, that the condition reported by Holle *et al.*²³ is not geographic retinal dysplasia, but rather a separate unknown condition that occurs after retinal development has occurred.

Retinal dysplasia commonly occurs concurrently with other idiopathic or inherited congenital ocular anomalies. The English Springer Spaniel⁵ and Yorkshire Terrier¹⁴ are reported to have the condition in association with cataracts, while the Sealyham Terrier⁷, Bedlington Terrier², Labrador Retriever^{13, 27}, and Akita¹² are reported to have retinal dysplasia in association with cataracts and microphthalmia. In the Labrador Retriever retinal dysplasia may also be associated with persistent pupillary membranes¹³ and

skeletal dysplasia^{26, 27}. In the Doberman Pinscher an autosomal recessive inherited congenital anomaly is reported that is characterized by microphthalmia, retinal dysplasia and anterior segment dysgenesis.^{11, 28-30} Multiple ocular defects including microphthalmia, cataracts, lenticonus with lens capsule rupture, persistent pupillary membranes, goniodysplasia, persistent hyperplastic tunica vasculosa lentis and persistent hyperplastic primary vitreous (PHTVL/PHPV) in association with retinal dysplasia is reported in Bloodhound puppies.⁶ Similarly, multiple ocular congenital defects including microphthalmia, buphthalmia, anterior synechia, acorea and aphakia in association with retinal dysplasia is reported in Saint Bernard puppies.¹⁷ Most recently, retinal dysplasia associated with persistent hyperplastic primary vitreous (PHPV) is reported in the Miniature Schnauzer dog.¹⁵ Although the Chow-Chow and Australian Shepherd dog have been cited as having retinal dysplasia in conjunction with other ocular defects¹⁹, a histopathologic diagnosis of retinal dysplasia has not been confirmed in these breeds. Similarly, the Samoyed dog has been reported to have retinal dysplasia in conjunction with short-limbed dwarfism³¹ however, histopathologic evidence of retinal dysplasia was not demonstrated in the study.

HISTOPATHOLOGY

Histopathology is necessary to confirm a diagnosis of retinal dysplasia. Histologically retinal dysplasia is characterized by folding of the neuroepithelium and the formation of rosettes in the sensory retina.³² (Figure 3) Lahav *et al.*³² describe four types of rosettes: (i) Three-layer rosettes which have the appearance of mature retina that has been secondarily thrown into folds; (ii) Two-layer rosettes in which the innermost layer resembles a photoreceptor cell layer with external limiting membrane and a large lumen containing undifferentiated cells. Surrounding these is a more peripheral layer of bipolar-like cells or poorly differentiated cells; (iii) One-layer rosettes with a single layer of moderately well-differentiated neural cells, usually several cells thick, having a structure similar to an external limiting membrane and surrounding a lumen. Within the lumen larger undifferentiated cells containing pigment granules are often observed; (iv) Primitive unilayer rosettes in which a single layer of undifferentiated retinal cells surround a lumen

delineated by an external membrane-like structure or, groups of cells that are arranged in a circle with a central tangle of fibrils.³² Many rosettes examined Lahav *et al.*³² appeared to have developed from the outer nuclear layer of the retina but the degree of disorganization prevents definitive determination of the layer of origin.³² Other common concurrent histologic examination findings include retinal folds, retinal detachment or non-attachment, persistent hyperplastic primary vitreous and retinal pigment epithelium hypertrophy and hyperplasia.^{9, 20, 32} Some retinal folds are not true dysplasia. These folds are believed to be caused by a transient growth differential between the inner and outer layers of the optic cup.³³ While folds may be encountered as a component of retinal dysplasia, they are distinct in terms of pathogenesis and significance.³³ The distinction between these retinal folds and retinal dysplasia is difficult to make ophthalmoscopically, thus requiring histopathology to differentiate between the two conditions. Retinal folds due to growth differential may disappear as the animal matures while retinal dysplasia represents permanent retinal pathology.³⁴

ETIOLOGY

Etiologies for retinal dysplasia in dogs include genetic mutations¹⁵, viruses³⁵ and irradiation.³⁶ The condition is proven to be inherited as an autosomal recessive trait in the Miniature Schnauzer dog¹⁵, English Springer Spaniel²⁴, American Cocker Spaniel⁹, Bedlington Terrier³ and Golden Retriever.³⁷ Limited pedigree analysis in the Yorkshire Terrier is also suggestive of autosomal recessive inheritance.¹⁴ Retinal dysplasia associated with skeletal dysplasia in Labrador Retrievers has an autosomal dominant mode of inheritance with incomplete penetrance.²⁶

Although inheritance of retinal dysplasia appears to be the most important etiologic factor¹⁹, viral-³⁵; or radiation-³⁶ induced retinal dysplasia have also been reported in the dog. Experimental studies in neonatal puppies demonstrated that inoculation of herpes virus at 1 to 4 days postnatally induces systemic infection and panuveitis with retinal rosettes noted histopathologically.³⁵ The susceptibility of the retina to irradiation has also been demonstrated experimentally, such that irradiation of the immature dog retina leads to retinal rosette formation.³⁶ Retinal dysplasia in these cases is due to disorganization and

abortive repair rather than a true dysgenesis.³⁸ Viral etiologies of retinal dysplasia can be differentiated from inherited etiologies histologically. Retinal rosettes are demonstrated in all cases, however, the acute viral histologic lesions demonstrate nonsuppurative endophthalmitis with multifocal chorioretinal necrosis, and the chronic viral lesions demonstrate multifocal chorioretinal scarring and atrophy.³³ Also, with viral infection, the lesions may be prevalent in any part of the fundus, not just centrally as in the typical hereditary forms.¹⁹ Retinal dysplasia due to toxin exposure³⁹ and vitamin A^{40, 41}, taurine and zinc deficiency⁴² has been reported in other species. Although not documented in the dog, it is likely that these etiologies would also induce retinal dysplasia in this species.

PATHOGENESIS

The pathogenesis of retinal dysplasia is complex. Silverstein *et al.*³⁸ divided the pathogenesis into four categories: (i) a hyperplastic extension of the retina into abnormal sites away from the retinal pigment epithelium (RPE); (ii) secondary to retinal detachment from the RPE; (iii) over regions devoid of RPE, i.e. colobomas; and (iv) an *in situ* dysplasia in which the retina has never been separated from the RPE.³⁸ Based on the first three categories it is suggested that healthy RPE is an essential prerequisite for normal development of the retina. Detachment of the neural retina from the RPE or damage to the RPE during development results in the loss of cell organization with consequent abnormal retinal development. The retinal dysplasia *in situ* has been shown to occur with bluetongue virus infection in lambs. This category of retinal dysplasia is thought to result from a necrotizing inflammatory response of the retina to infection, resulting in disorganization and abortive repair rather than true dysgenesis.³⁸ Silverstein's hypothesis is supported by a study in Doberman Pinschers on congenital blindness with ocular developmental anomalies.²⁸ In this study a highly abnormal retinal pigment epithelium was evident and thus it was proposed that the RPE may play a role in the pathogenesis of retinal dysplasia in this breed. In most breeds, however, the pathogenesis of retinal dysplasia remains to be elucidated.

RECENT DISCOVERIES IN RETINAL DYSPLASIA

The molecular basis of inherited retinal dysplasia in Miniature Schnauzer dog has recently been investigated.⁴³ Using a complementary deoxyribonucleic (cDNA) pool of retinal and RPE tissue from an affected and unaffected dog, representational difference analysis (RDA) was performed to identify candidate genes causing the disease. The RDA test provided evidence of altered mitochondrial deoxyribonucleic acid (mtDNA) or mitochondrial transcription activity in affected Miniature Schnauzer dog retina and RPE. To confirm these findings, real-time polymerase chain reaction (PCR) was performed to make quantitative measurements of white blood cell mtDNA, and retinal and RPE mRNA transcript levels, of an affected and normal dog. Results from the real-time PCR revealed that the affected dog had decreased mtDNA and mRNA expression of several mitochondrial genes in retinal and RPE tissues along with approximately 30% less white blood cell mtDNA.⁴³ As mitochondrial mutations are maternally inherited and the inheritance of retinal dysplasia in Miniature Schnauzer dogs is autosomal recessive¹⁵, a mutation in a nuclear-encoded gene that affects mtDNA transcription was suspected.⁴³ *Tfam* is a nuclear encoded gene that controls DNA transcription and copy number.⁴⁴ Using real-time PCR Appleyard *et al.*⁴³ measured *Tfam* expression in affected and normal dogs and in correspondence with the decreased mtDNA and mRNA, *Tfam* mRNA levels were also decreased in the retina and RPE of the affected dog. Based on these findings it was proposed that the pathogenesis of retinal dysplasia may be due to a decreased energy supply to the retina and RPE during development.⁴³ These molecular findings also led the authors to examine mitochondrial morphology from neutrophils, skeletal muscle, semen epithelial cells and spermatozoa using transmission electron microscopy. The mitochondria from the affected dogs appeared reduced in size and number and appeared to have an abnormal structure in all the tissues examined. Morphologically, the number of cristae within each mitochondrion appeared reduced and there was poor definition of the characteristic double cristal membrane.⁴³ (Figures 4 and 5)

STUDY OBJECTIVES

This study of retinal dysplasia was undertaken to further investigate the pathogenesis of retinal dysplasia in Miniature Schnauzer and English Springer Spaniel dogs. The objectives of this study are to:

- a) determine if there are mutations in the *Tfam* promoter, intron1, structural gene sequence and 3' non-coding region in Miniature Schnauzer dogs affected with retinal dysplasia and occasionally expressed PHPV; and to quantitate and measure the surface area of lymphocyte mitochondria, and compare mitochondrial morphology between affected and normal Miniature Schnauzer dogs using electron microscopy
- b) determine if English Springer Spaniel dogs affected with retinal dysplasia have decreased leukocyte mtDNA compared to normal dogs and to quantitate and measure the surface area of lymphocyte mitochondria, and compare mitochondrial morphology between affected and normal English Springer Spaniel dogs using electron microscopy.

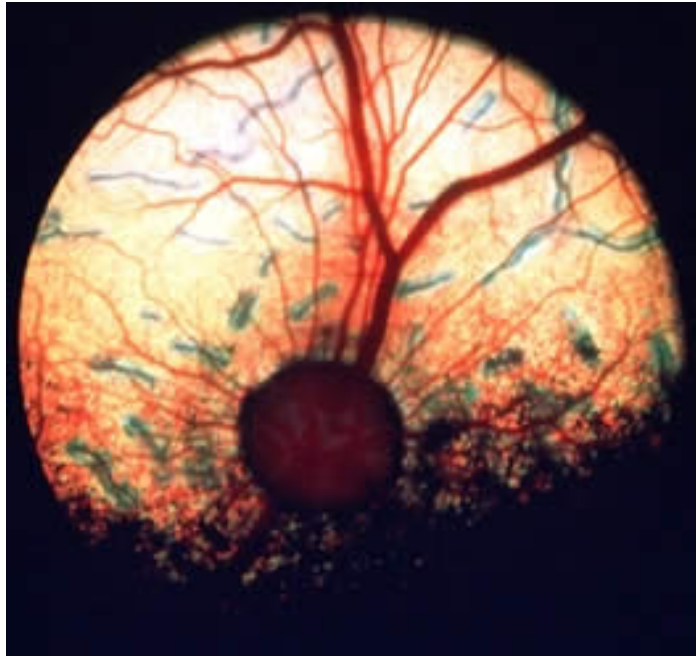


Figure 1. Multifocal retinal dysplasia with several grey, hyporeflective streaks and lines evident in the tapetal fundus. Photo courtesy of B. H. Grahn.



Figure 2. Geographic retinal dysplasia with the typical horse-shoe shaped fundic lesion in the tapetal fundus. Hyperreflective areas are indicative of retinal thinning. Photo courtesy of B. H. Grahn.

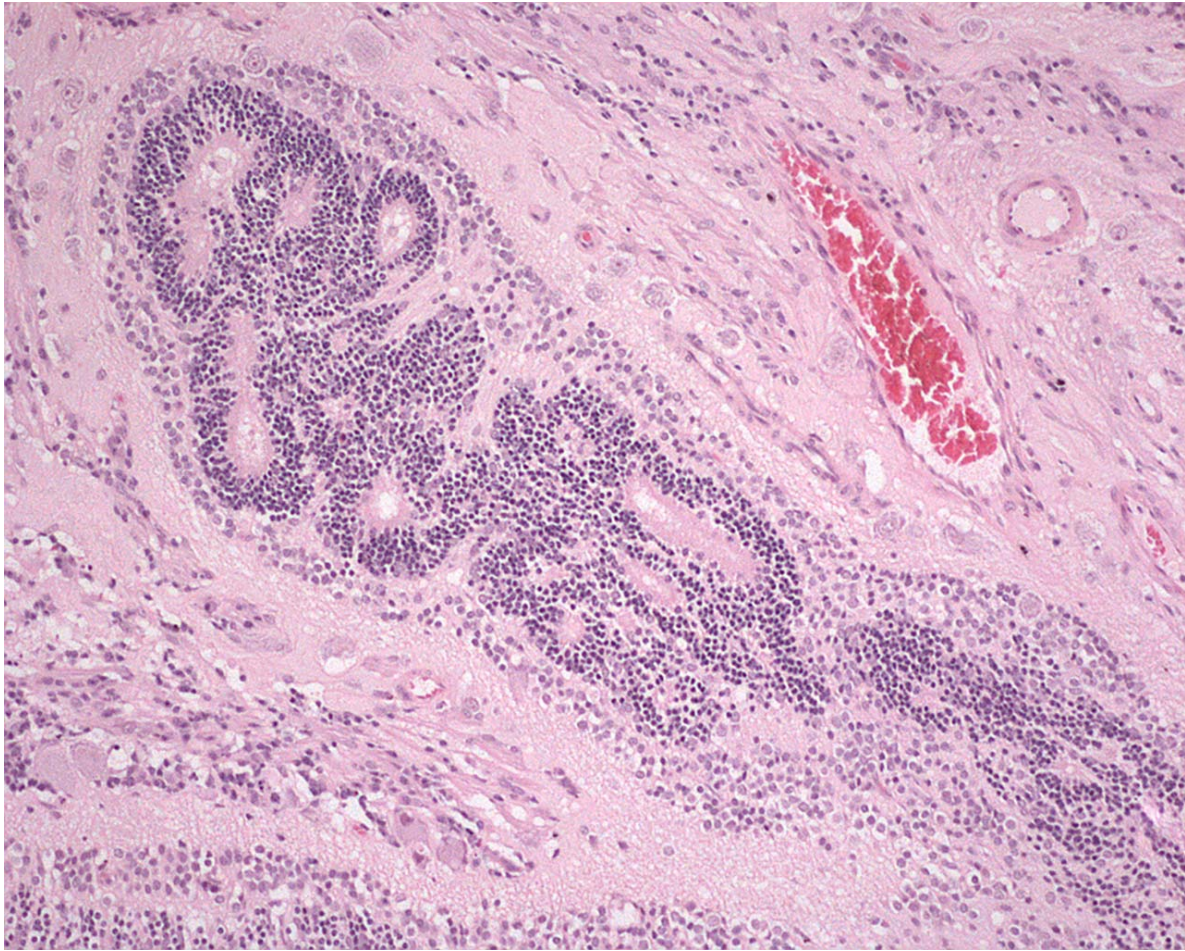


Figure 3. A hematoxylin and eosin-stained histologic section of a retina from a Miniature Schnauzer dog with inherited retinal dysplasia. Rosettes composed of a central lumen containing dysplastic photoreceptor inner and outer segments are evident. Photo courtesy of B. H. Grahn.

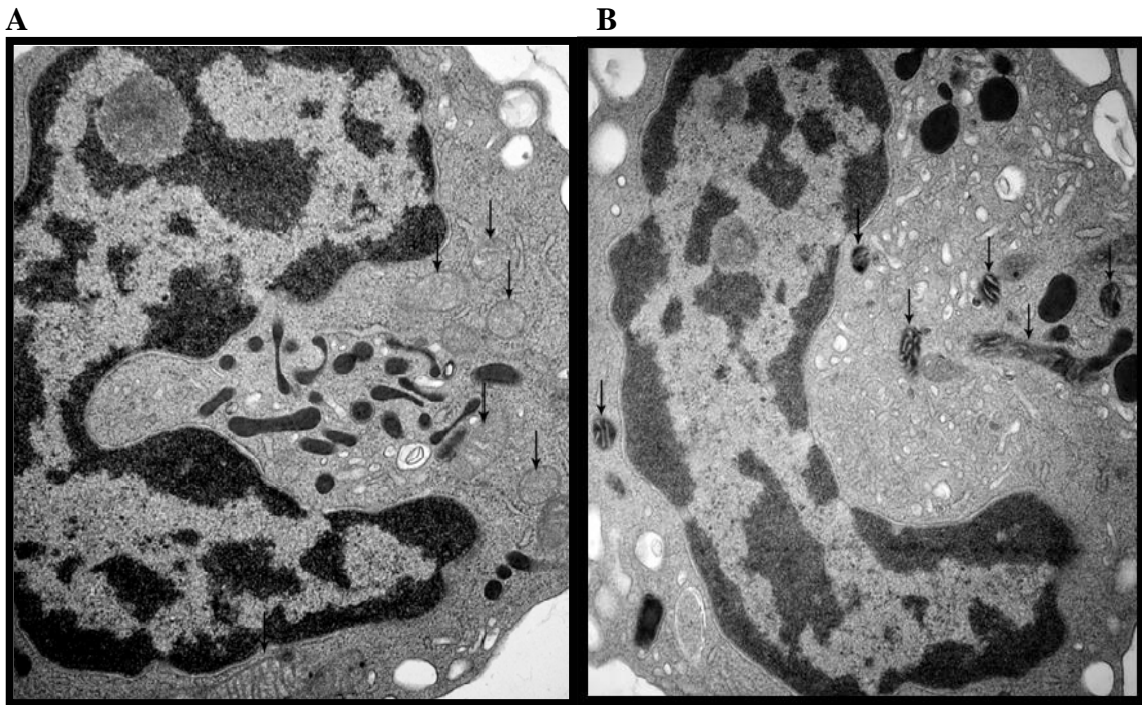


Figure 4. Transmission electron micrographs of a neutrophil from a normal Miniature Schnauzer dog (**A**) and a Miniature Schnauzer dog affected with retinal dysplasia (**B**). The mitochondria of the affected dog appear reduced in size and number and are more electron dense compared to the normal dog. *Arrows:* mitochondria. Magnification x 18,000. Reprinted by permission from The Association for Research in Vision and Ophthalmology: Appleyard, G.D., G.W. Forsyth, L.M. Kiehlbauch, *et al.*, *Differential mitochondrial DNA and gene expression in inherited retinal dysplasia in Miniature Schnauzer dogs*. Invest Ophth Vis Sci, 2006. **47**(5): p. 1810-6, copyright (2006).

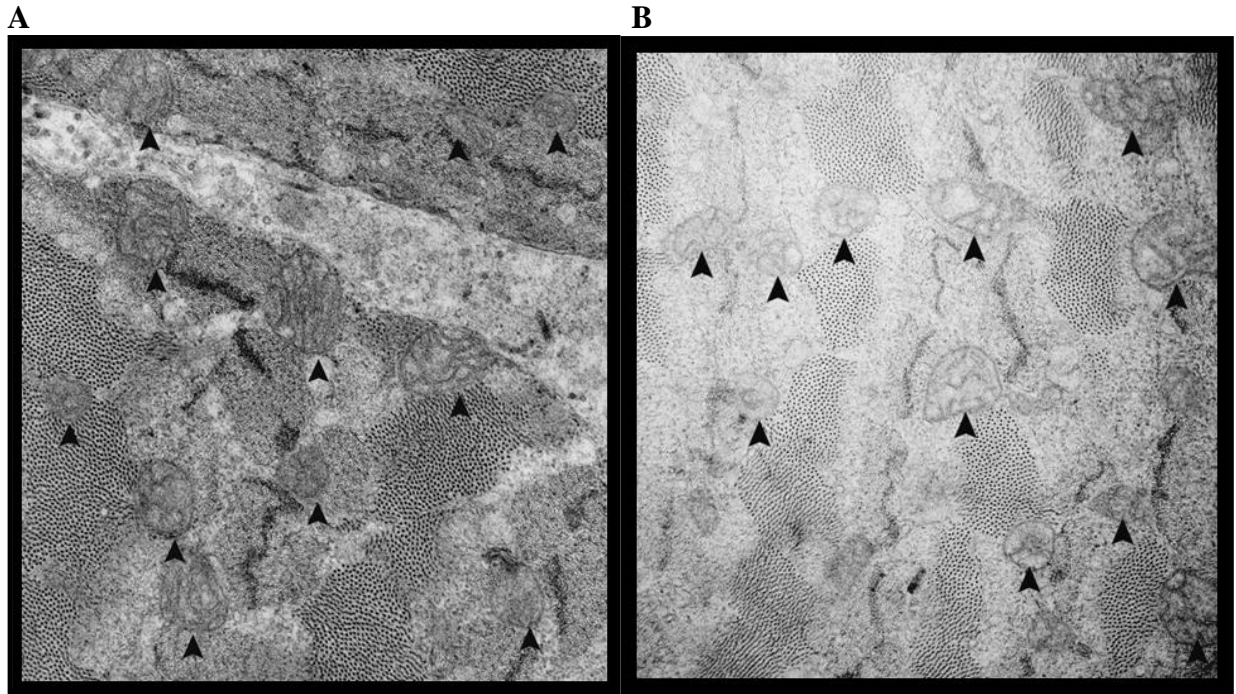


Figure 5. Transmission electron micrographs of skeletal muscle from a normal Miniature Schnauzer dog (**A**) and a Miniature Schnauzer dog affected with retinal dysplasia (**B**). The mitochondria of the affected dog appear reduced in size and number and the cristae appear abnormal compared to the normal dog. *Arrowheads*: mitochondria. Magnification x 18,000. Reprinted by permission from The Association for Research in Vision and Ophthalmology: Appleyard, G.D., G.W. Forsyth, L.M. Kiehlbauch, *et al.*, *Differential mitochondrial DNA and gene expression in inherited retinal dysplasia in Miniature Schnauzer dogs*. Invest Ophth Vis Sci, 2006. **47**(5): p. 1810-6, copyright (2006).

GENERAL LITERATURE REVIEW

SECTION 1

REGULATION OF NUCLEAR GENE EXPRESSION

The first level of regulation of differential gene expression occurs at the initiation of messenger ribonucleic acid (mRNA) synthesis from the DNA template. The frequency of initiation depends on sequence-specific transcription factors that activate or repress transcription from the gene.⁴⁵ The control region in the immediate vicinity of a transcription start site is called the promoter; which specifically binds ribonucleic acid (RNA) polymerase along with other transcription factors and determines where transcription begins.⁴⁶ Transcription of genes can also be stimulated by enhancer sequences, which can regulate a promoter from a distance and in an orientation-independent fashion.⁴⁵

Most vertebrate genes contain introns which are non-protein encoding sequences of DNA. The introns are transcribed but are precisely excised from primary transcripts to form mature mRNAs with continuous message.⁴⁶ Certain genes have been demonstrated to have DNA-binding protein sites or transcription factor binding sites situated in introns that stimulate or inhibit gene transcription. These binding sites are situated primarily in the first intron (intron 1)⁴⁷⁻⁴⁹, although in some cases they can be situated in other introns.⁵⁰ Thus, DNA-binding proteins can mediate a complex set of interactions between intronic and 5' flanking promoter sequences which in turn, can aid in gene transcription regulation.⁴⁸

NUCLEAR GENE TRANSCRIPTION AND POLYADENYLATION

RNA polymerase II requires other transcription factors collectively known as TFII to form a complex and initiate transcription.⁴⁶ RNA polymerase proceeds along the DNA template and transcribes until a terminator sequence is reached. Primary transcripts are then cleaved by a specific endonuclease that recognizes the sequence AAUAAA (known as

the polyadenylation site).⁵¹ Cleavage does not occur if the polyadenylation site or a segment of some 20 nucleotides on its 3' side is deleted.⁴⁶ After cleavage by the endonuclease, most pre-mRNAs are polyadenylated in which a poly(A) polymerase adds approximately 250 A residues to the 3' end of the transcript.⁵² Mutations that disrupt the process of polyadenylation have been demonstrated to result in decreased mRNA levels.^{53,}

54

MITOCHONDRIAL GENETICS

Mitochondria are the energy-transducing organelles of eukaryotic cells with their principle function being adenosine-5'-triphosphate (ATP) production through electron transfer and oxidative phosphorylation.⁵⁵ Morphologically, mitochondria have a double membrane; the outer membrane separates the mitochondrion from the cytosol and the inner membrane is invaginated to form the cristae which protrude into and define the matrix of the organelle.⁵⁶ Five discrete multi-subunit enzyme complexes are embedded in the inner mitochondrial membrane and catalyze electron transfer from respiratory chain substrates to oxygen.⁵⁵ This electron transfer results in the translocation of protons and production of protonic energy which is utilized for ATP synthesis, ion translocation and protein importation.⁵⁵ The five enzymes complexes that make up the oxidative phosphorylation system are: NADH:ubiquinone oxidoreductase (complex I); succinate:ubiquinone oxidoreductase (complex II); ubiquinol:ferricytochrome *c* oxidoreductase (complex III); ferrocytochrome *c*:oxygen oxidoreductase (complex IV); and ATP synthase (complex V).⁵⁵

Mitochondria contain their own genome, mitochondrial DNA (mtDNA), which is located in the mitochondrial matrix⁵⁷ and makes up approximately 1% of a cell's total DNA population.⁵⁸ The maintenance of mtDNA integrity is essential for normal function of the respiratory chain and thus ATP production.⁵⁹ In mammalian cells, mitochondrial genes are present at high copy number (usually 10^3 - 10^4 copies/cell)⁶⁰ with 2-10 copies of mtDNA existing within each mitochondrion.^{61, 62} Regulation of mtDNA copy number is important for maintaining mitochondrial ATP production, as the level of mtDNA transcripts largely depends on the copy number of mtDNA.⁵⁹

Mammalian mtDNA is a maternally inherited circular double stranded molecule that in most species, including the canine, encodes 13 essential polypeptides involved in the respiratory chain-oxidative phosphorylation system along with two ribosomal ribonucleic acid (rRNA) subunits and 22 transfer ribonucleic acid (tRNA) molecules involved in mitochondrial translation.⁶³ The length of the mtDNA molecule in the canine is 16,728 base pairs (bp) and the organization and direction of the open reading frames and the regulatory control region are the same as those in other mammalian species.⁶³ (Figure 1) The mitochondrial-encoded respiratory chain proteins reside mainly in the inner mitochondrial membrane.⁶⁴ The remainder of the respiratory chain-oxidative phosphorylation system subunits and all the proteins required for the replication and transcription of mtDNA are nuclear-encoded. These nuclear-encoded proteins are therefore synthesized in the cytosol and imported into the mitochondria where they are either linked to mtDNA transcription/replication or they are co-assembled with the mtDNA-encoded subunits into respiratory chain complexes. Thus, the function of the respiratory chain and mtDNA maintenance is regulated by both mitochondrial and nuclear genes.⁶⁵ The individual strands of mtDNA are denoted heavy (H) and light (L) strands as they have different buoyant densities in a cesium chloride gradient. The mitochondrial genome lacks introns however; a long non-coding regulatory region, known as the displacement-loop (D-loop), exists within the genome and initiation of transcription occurs from two major promoters within the D-loop, the light- and heavy-strand promoters (LSP and HSP).⁶⁶ (Figure 1) Transcription from LSP is necessary not only for gene expression but also for production of RNA primers required for initiation of mtDNA replication. Thus, transcription is a prerequisite for mtDNA replication.⁶⁶

Mitochondria are dynamic organelles that respond to developmental and environmental signals in meeting cellular energy demands.⁶⁷⁻⁶⁹ The regulation of mtDNA transcription is of fundamental importance for maintaining metabolic functions in the eukaryotic cell, however, little is known about the mechanisms of mitochondrial transcription and how the levels of transcription are regulated in response to metabolic need.

MITOCHONDRIAL TRANSCRIPTION AND TRANSCRIPTION FACTOR A (TFAM)

Transcription factor A (TFAM) is a nuclear encoded protein factor that is encoded by the *Tfam* gene.⁷⁰ In canines, the *Tfam* gene maps to chromosome 4 and is a 13,379 nucleotide sequence made of up 7 exons which encode a polypeptide of 246 amino acids.⁷¹ (Figure 2) Structurally, *Tfam* possesses two high mobility group (HMG) boxes which are sequences of DNA that are considered to be involved in DNA binding⁷⁰, and a C-terminal tail composed of 25 amino acids.⁷² The protein binds to elements in both heavy- and light strand promoters on mtDNA and appears to be the principal activator of transcription by the mitochondrial RNA polymerase.⁷³ Although TFAM has a higher affinity to the LSP and HSP promoters on mtDNA, it also has nonspecific DNA-binding activity irrespective of DNA sequence.^{74, 75} TFAM also has a role in mtDNA replication, since transcription generates an RNA primer necessary for initiation of mtDNA replication.⁶⁶ As TFAM is abundant in mammalian mitochondria with a molar ratio of TFAM to mtDNA of ~900-1000:1⁷⁶, it is likely that mammalian mtDNA is fully covered with TFAM protein and that TFAM is also a major component in the formation of the nucleoid structure helping stabilize mtDNA.^{59, 76}

The current general model for human mitochondrial transcription is that TFAM binds to LSP and then recruits mitochondrial RNA polymerase (POLRMT) and the mitochondrial transcription factor B paralogues, TFB1M and TFB2M to initiate the transcription process.⁷⁷⁻⁷⁹ It is speculated that the initial TFAM binding introduces specific structural alterations in mtDNA (i.e. unwinding of the promoter region) which can facilitate promoter recognition by the TFBM/POLRMT complex.^{60, 80} The C-terminal tail of TFAM has an essential role in the initiation of the promoter-specific transcription *in vitro*⁷², as it has been demonstrated to be responsible for the binding of TFAM to TFBM⁸¹ and to strengthen the general binding of TFAM to DNA.⁸² TFAM is known to control mitochondrial transcription activity and copy number and it has been demonstrated *in vivo* that the protein is necessary for mtDNA maintenance and embryogenesis in mice.⁴⁴ Larsson *et al.*⁴⁴ demonstrated that heterozygous knockout mice (+/*Tfam*⁻) have reduced mtDNA copy number, reduced mitochondrial transcription and a respiratory chain

dysfunction in the heart. In these mice, the mtDNA copy number decreased by 34+/- 7% in all tissues analyzed, and the mitochondrial transcript numbers were reduced by 22+/- 10% in heart and kidney. Homozygous knockout embryos (*Tfam*⁻/*Tfam*⁻) exhibited severe mtDNA depletion with abolished oxidative phosphorylation and abundant enlarged mitochondria with abnormal cristae. (Figure 3) These embryos proceeded through implantation and gastrulation but exhibited growth retardation, delayed neural and cardiac development and died prior to embryonic day E10.⁴⁴ Further studies in mice⁸³, chicken⁸⁴ and human cells⁵⁹ have also demonstrated TFAM to be a major determinant of mtDNA amount and that mtDNA copy number is directly proportional to the total TFAM protein levels in mouse embryos.⁸³ Moreover, targeted disruption of *Tfam* in cardiac myocytes induced deletion of mtDNA and mitochondrial transcripts leading to dilated cardiomyopathy.^{85, 86} A reduction of TFAM expression has been demonstrated in cardiac failure and overexpression of TFAM can prevent the decline in mtDNA as well as mitochondrial respiratory defects in post-myocardial infarction hearts.⁸⁷ These lines of evidence have established a critical role for TFAM in the regulation of mtDNA copy number and transcription as well as in the maintenance of mitochondrial physiological function.

THE POLYMERASE CHAIN REACTION

The polymerase chain reaction (PCR) is a method which allows exponential amplification of specific DNA sequences.⁸⁸ The technique was developed by Kary Mullis in 1984 and has since been an invaluable tool for DNA manipulation.⁸⁹ The requirements for PCR include a DNA polymerase, a pair of oligonucleotide primers, deoxyribonucleoside triphosphates (dNTPs), a template and a buffer containing magnesium.⁸⁸

The most commonly used DNA polymerase is Taq polymerase. The enzyme is derived from the organism *Thermus aquaticus* and its advantages of heat stability and high temperature optimum make it the ideal choice for use as a DNA polymerase in PCR.⁹⁰ A pair of synthetic oligonucleotide primers are necessary to prime DNA synthesis. The design of these primers is crucial to the efficiency and specificity of the amplification

reaction.⁸⁸ The primers are designed complementary to the DNA regions at the 5' and 3' ends of the DNA region to be amplified.⁹⁰ If all nucleotides are randomly distributed in any given DNA sequence the expected frequency of occurrence of a sequence (K) is given by the following equation:

$$K = [g / 2]^{G+C} \times [(1 - g) / 2]^{A+T} \quad [\text{Eq. 1}]$$

where G, C, A, T are the number of guanine, cytosine, adenosine, and thymidine nucleotides in the oligonucleotide, and g is the relative G+C content of the sequence.⁹¹ Based on this equation, a minimum oligonucleotide primer length of 17 is recommended to ensure uniqueness.⁹⁰ Primer sequences should also have minimal secondary structure, no significant sequence identity with other sequences of the target genome and low complementarity to each other, particularly in the 3' region.⁸⁸ The specificity of PCR also depends strongly on the melting temperature (T_m) of the primers.⁸⁸ The T_m is the temperature at which half of the primer has annealed to the template.⁸⁸ Best results are obtained when the melting temperatures are similar for both primers.⁸⁸ The dNTPs are the nucleotide bases from which the DNA polymerase synthesizes a new DNA strand and include deoxyadenosine triphosphate (dATP), deoxythymidine triphosphate (dTTP), deoxycytidine triphosphate (dCTP), and deoxyguanosine triphosphate (dGTP). Standard PCRs contain equimolar amounts of dATP, dTTP, dCTP, and dGTP.⁸⁸ Lastly, a buffer solution and magnesium are essential for efficient DNA polymerase action and stability.⁹⁰

The process of PCR involves three essential steps: denaturation of the template by heat, annealing of the primers to the single-stranded target sequence, and extension of the annealed primers by a DNA polymerase.⁸⁸ These steps are carried out in a thermal cycler which controls the temperature required at each reaction step. The selection of temperatures and times depends on the DNA being amplified and the primers chosen.⁹⁰ The amplified products of PCR accumulate exponentially as described in Equation 2⁸⁸:

$$N_f = N_o (1 + Y)^n \quad [\text{Eq. 2}]$$

where N_f is the final copy of amplified sequence after n cycles of amplification, N_0 is the initial copy number of the target sequence in the DNA template and Y is the efficiency of amplification per cycle. The efficiency of PCR is determined predominately by the quality of the DNA polymerase, and in the exponential phase of the reaction efficiency can be calculated from Equation 3⁸⁸:

$$Y = \left[\frac{N_f}{N_0} \right]^{1/n} - 1 \quad [\text{Eq. 3}]$$

where Y is the efficiency of amplification per cycle, N_0 is the initial copy number of the target sequence in the DNA template and N_f is the number of amplified molecules produced in n cycles of exponential amplification. The exponential phase of amplification continues until one of the reaction components becomes limited or accumulating products decrease efficiency.⁸⁸

Certain target DNA sequences can be more difficult to amplify than others; especially for templates with high GC content.⁹² This can often be overcome by alteration of the PCR technique or reagents.⁹² The product(s) obtained from PCR should be a defined length. When PCR is complete, the product and appropriate molecular-weight markers are loaded onto an agarose gel containing ethidium bromide for electrophoresis and are then visualized by ultraviolet transillumination.⁹⁰

SECTION 2

RETINAL DYSPLASIA IN THE ENGLISH SPRINGER SPANIEL DOG

Retinal dysplasia has been well studied in the English Springer Spaniel with ophthalmoscopic, light, and transmission electron microscopic findings being well documented in this breed.^{1, 5, 20, 22, 93-96} The condition has its morphogenic inception in the English Springer Spaniel between days 45 and 50 of gestation.^{1, 22, 94, 97} At day 46 of gestation, a marked decrease in the size and area occupied by the gap junctions within the external limiting membrane of dysplastic fetal eyes is evident when compared to normal fetuses.⁹⁴ By day 50-55 of gestation, and at days 1 and 7 postnatally, the rosettes formed by neuroblasts have a central lumen with a distinct external limiting membrane.¹ The folds occasionally progress to focal retinal detachment and associated RPE hypertrophy.¹ Histologically, the retinal rosettes are present at birth and located primarily in the peripapillary tapetal retina.^{1, 20, 98} A discrete external limiting membrane is absent in the dysplastic areas.²⁰ Ultrastructurally in the dysplastic areas, the Müller cell radial processes are either absent or disorganized.²² From day 45 of gestation to postnatal day one, deep (sclerad) aberrant retinal vessels are often noted within the lumens of rosettes and folds however, the continuity of these vessels with choroidal or retinal vessels has not been determined.²⁰ Abnormal intravitreal vessels can also develop concurrently with fold-rosette complexes in the English Springer Spaniel.^{20, 98} The dysplastic lesions are non-progressive but secondary retinal detachment is occasionally noted and retinal atrophy within the region of dysplasia is relatively common in dogs older than two years of age.²⁰

Histological evaluations of the English Springer Spaniel dysplastic retinas have failed to show evidence of inappropriate retinal pigment epithelium development. Thus, O'Toole *et al.*²⁰ believe that Silverstein's⁹⁹ proposed pathologic mechanisms of retinal dysplasia do not appear to have relevance to the development of heritable retinal dysplasia in this breed. Based on the light microscopic and ultrastructural findings by O'Toole *et al.*^{20, 22}, two further mechanisms of retinal dysplasia have been proposed. As abnormal intravitreal and intraretinal vessels develop concurrently with fold-rosette complexes in the English Springer Spaniel fetuses, O'Toole *et al.*^{20, 22} propose that the retinal dysplasia may

occur secondarily to inappropriate development of the hyaloid and retinal vascular systems. The studies by O'Toole *et al.*^{20, 22} also demonstrated the presence of disorganized Müller fibres within the dysplastic areas and the focal absence of a discrete external limiting membrane. Müller cells are thought to act as a scaffold for neuroblast migration.¹⁰⁰ Based on these findings it has been proposed that retinal dysplasia could also be due to the defective development of Müller cells or abnormal gliovascular relationships leading to abnormal differentiation and migration of neuroblasts.^{20, 98} O'Toole *et al.*²² believe that these mechanisms may also explain other aspects of this disease, including retinal detachment and persistence of the hyaloid vasculature.^{20, 98}

Based on the findings of decreased gap junction size and area within the external limiting membrane⁹⁴, Whiteley¹ has proposed that inappropriate expression of cell adhesion molecules or glycoproteins on the neuroepithelium or Müller cells may lead to poor cell adhesion. This, in turn may lead to the inability to form cell junctions or proper cell-cell communication, causing subsequent disorganized proliferation of neuroblasts.¹ Due to these particular morphologic findings, further studies by Whiteley *et al.*¹⁰¹ investigated the role of membrane proteins known as intramembranous particles (IMP) and the ability of membrane probes (filipin in particular) to bind cell membranes.¹⁰¹ Differences in intramembranous particle density and filipin binding were identified in affected English Springer Spaniel dogs compared to age-matched controls.¹⁰¹ Based on these findings, Whiteley *et al.*¹⁰¹ suggest that abnormalities in the membrane structure of neuroblastic cells may be related to the dysplastic process.¹⁰¹

REAL-TIME POLYMERASE CHAIN REACTION (PCR)

Real-time polymerase chain reaction (PCR) is the method of choice to quantify nucleic acids.⁸⁹ It is based on the revolutionary method of PCR which amplifies specific pieces of DNA however; real-time PCR allows quantification of PCR products as they are generated.⁸⁹ Fluorescent reporter dyes emit fluorescence when bound to double stranded DNA (dsDNA) and the fluorescence intensity increases proportionally to the dsDNA concentration. During amplification, the cycle at which the fluorescent signal reaches a threshold level (known as C_T) correlates with the amount of original target sequence,

thereby enabling quantification. This C_T value is inversely proportional to the amount of specific nucleic acid sequence in the original sample.¹⁰² (Figure 4) The threshold fluorescence level is determined as significant fluorescence above a calculated background fluorescence.¹⁰³ The final product from any unique pair of primers on a target gene can be further characterized by subjecting it to increasing temperatures to determine when the double-stranded product becomes single stranded. This melting point is a unique property dependent on product length and nucleotide composition.⁸⁹ (Figure 5)

To correct for sample-to-sample variation in the amount of DNA template simultaneous amplification of an internal reference gene is performed. This reference gene serves as an internal reference against which other values can be normalized as it is expressed at a constant level among different tissues of an organism and at all stages of development. The most commonly used reference genes include glyceraldehyde-3-phosphate-dehydrogenase (GA-3-PDH) and β -actin.¹⁰² In order to ensure reproducibility, all assays are run in triplicate and should be repeated at least once.¹⁰³ Amplification efficiency of the reactions performed is an important consideration in relative quantitation.¹⁰⁴ The efficiency is influenced by the template GC content, length of the amplified product, annealing temperature and secondary structure.¹⁰³ Amplification efficiency is calculated using data from a standard curve with the following formula¹⁰⁴:

$$\text{Efficiency} = [10^{(-1/\text{slope})}] \quad [\text{Eq. 4}]$$

Numerous mathematical models exist to calculate relative quantitation. When amplification efficiencies are similar in the target and reference genes being amplified the comparative C_T method can be used.¹⁰⁵ C_T values in the linear exponential phase of the target gene (COX-1) are normalized to the reference gene (GA-3-PDH) by calculating ΔC_T and then calibrated using the following equations¹⁰⁵:

$$\Delta C_T = C_{T \text{ target gene}} - C_{T \text{ reference gene}} \quad [\text{Eq. 5}]$$

$$\Delta \Delta C_T = \Delta C_{T \text{ sample}} - \Delta C_{T \text{ calibrator}} \quad [\text{Eq. 6}]$$

The amount of target, normalized to an endogenous reference and relative to a calibrator is then given by ¹⁰⁵:

$$R = 2^{-\Delta\Delta C_T} \quad [\text{Eq. 7}]$$

Another method of relative quantitation is based on the mathematical model by Pfaffl ¹⁰⁶ which corrects for changes in PCR efficiency. Equation 8 shows this model.

$$\text{Ratio} = \frac{(E_{\text{target gene}})^{\Delta C_{T \text{ target (calibrator-sample)}}}}{(E_{\text{reference gene}})^{\Delta C_{T \text{ reference (calibrator-sample)}}}} \quad [\text{Eq. 8}]$$

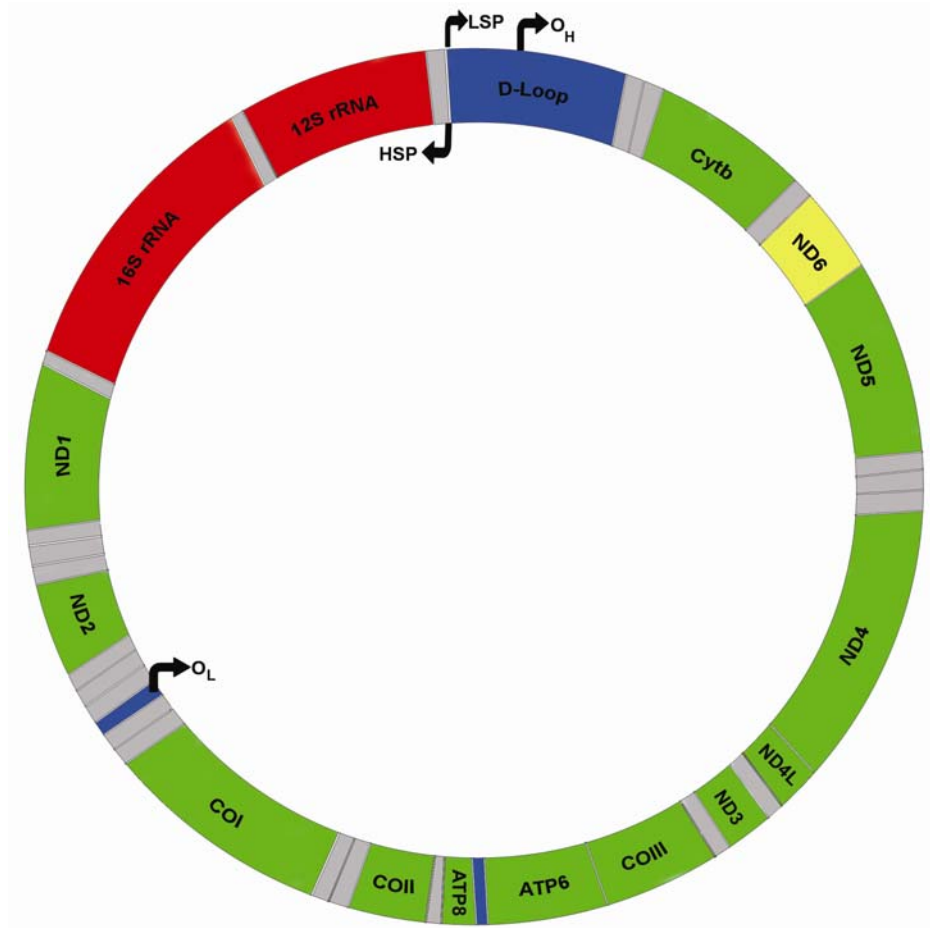


Figure 1. Map of the double-stranded mammalian mtDNA encoding the 13 proteins, 22 tRNAs and two rRNAs. Heavy-strand and light-strand origin of DNA replication occur at O_H and O_L, respectively. Heavy-strand transcription begins at the HSP. The HSP transcripts produce the 12S and 16S rRNAs (red) as well as 12 mRNA molecules (green) and tRNAs (grey). Transcription from the light-strand promoter (LSP) produces the mRNA molecule for ND6 (yellow) along with primers for the initiation of DNA synthesis. Non-coding regions are indicated in blue.

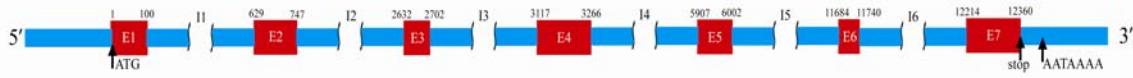


Figure 2. TFAM gene structure. Numbering is relative to the start codon. I = intron, E = exon.

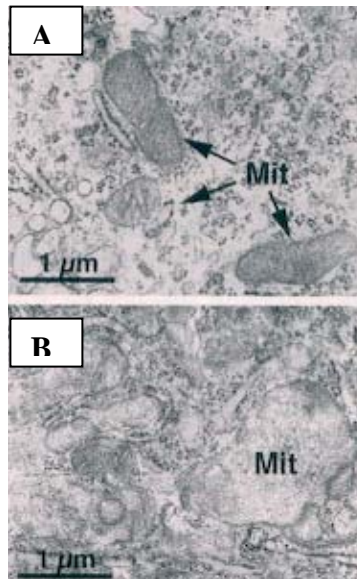


Figure 3. Electron micrographs of (A) control ($Tfam^+/Tfam^+$) and (B) homozygous knockout embryo ($Tfam^-/Tfam^-$) mitochondria exhibiting abundant enlarged mitochondria with abnormal cristae. Reprinted by permission from Macmillan Publishers Ltd: [NATURE GENETICS] (Larsson, N.G., et al., *Mitochondrial transcription factor A is necessary for mtDNA maintenance and embryogenesis in mice*. Nature Genetics, 1998. **18**(3): p. 231-6), copyright (1998).

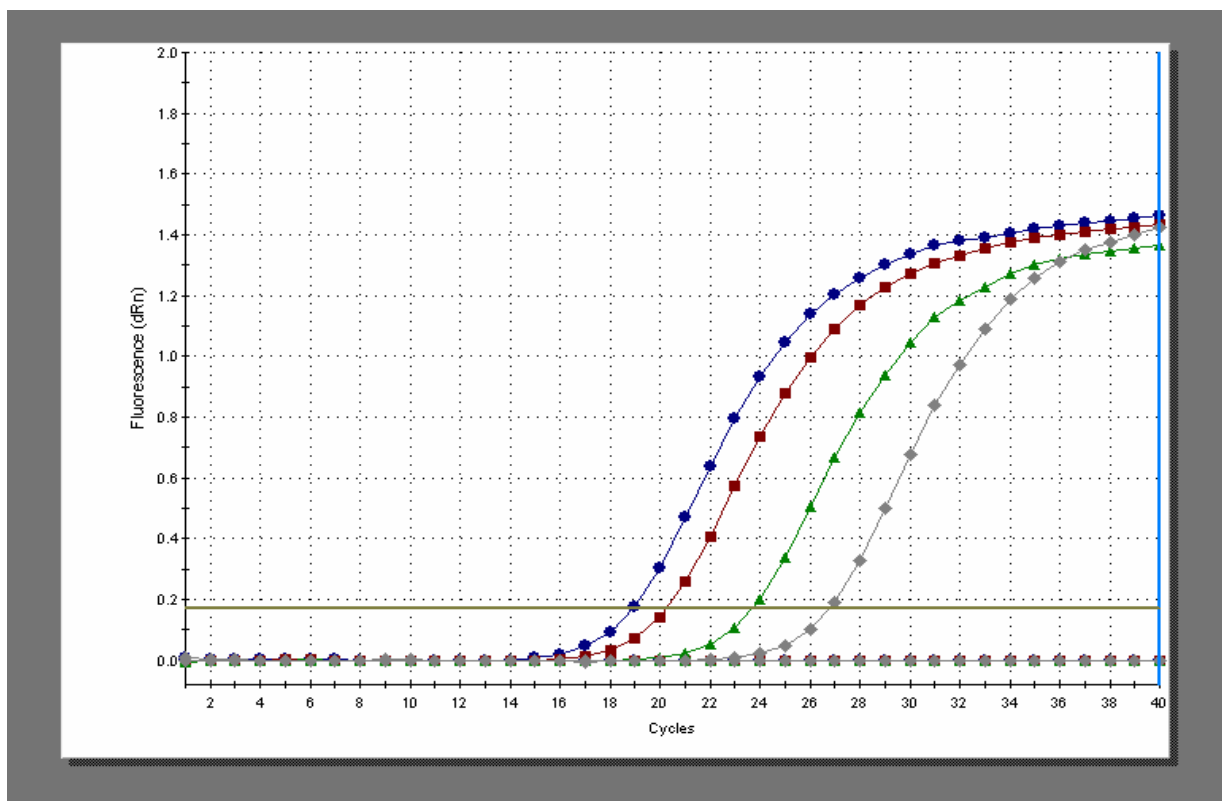


Figure 4. Real-time PCR amplification plots demonstrating cycles versus fluorescence for multiple DNA samples. The C_T value corresponds to the cycle at which fluorescence is determined to be statistically significant above the background and is inversely proportional to the amount of specific nucleic acid sequence in the sample. For the DNA sample marked $\bullet\text{---}\bullet\text{---}\bullet$ the C_T value is 19.

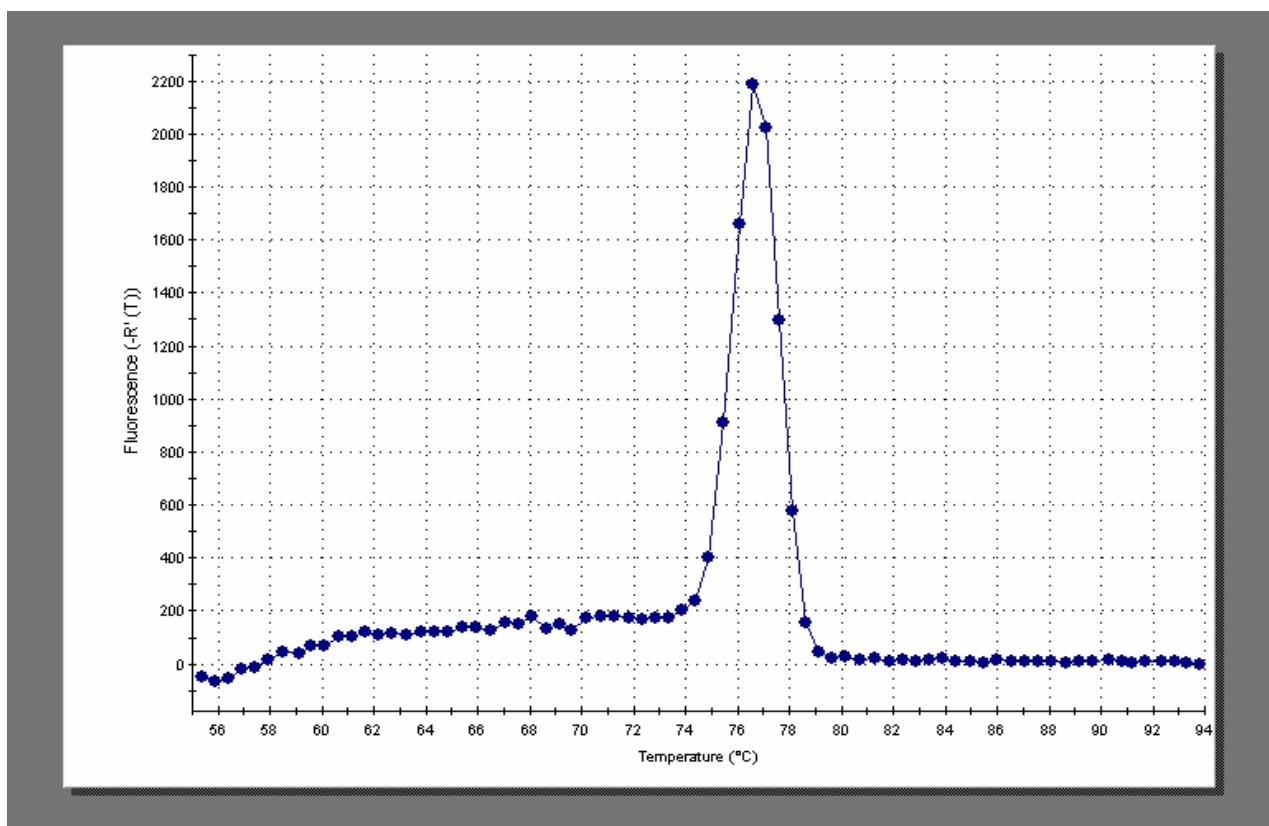


Figure 5. Dissociation analysis of a real-time amplicon. The negative derivative of fluorescence versus temperature was plotted against temperature. The curve shows a single, sharp peak, suggesting that only a specific PCR product was generated with this set of primers.

CHAPTER 1

NUCLEOTIDE SEQUENCING FOR THE MITOCHONDRIAL TRANSCRIPTION FACTOR A GENE (*Tfam*) AND LYMPHOCYTE MITOCHONDRIAL QUANTIFICATION AND MEASUREMENT IN MINIATURE SCHNAUZER DOGS AFFECTED WITH INHERITED RETINAL DYSPLASIA AND ASSOCIATED PERSISTENT HYPERPLASTIC PRIMARY VITREOUS

1.1 INTRODUCTION

Retinal dysplasia is defined as an abnormal differentiation of the outer layers of the retina.¹ The condition is a common congenital disorder in the dog and has been recognized in many breeds.⁴⁻¹⁶ The clinical manifestations of retinal dysplasia in the Miniature Schnauzer dog vary. Single or multiple retinal folds; geographic retinal dysplasia; and generalized dysplasia with retinal detachment have all been reported in the Miniature Schnauzer dog.^{15, 18, 107} Dysplastic lesions are usually most extensive dorsal to the optic disc involving the temporal and nasal retina.¹⁵ In this breed, persistent hyperplastic primary vitreous (PHPV) is present in approximately 20% of dogs affected with retinal dysplasia and the mode of inheritance of this syndrome has been determined to be autosomal recessive.¹⁵

The pathogenesis of retinal dysplasia is poorly understood and remains to be elucidated. The suspected etiology of retinal dysplasia in the Miniature Schnauzer dog is a genetic mutation as the condition is inherited as an autosomal recessive trait.¹⁵ Decreased mRNA expression of *Tfam*, a nuclear encoded gene controlling mitochondrial transcription and copy number, and of several mitochondrial genes in the retina and retinal pigment epithelium (RPE) of an affected Miniature Schnauzer dog has been described.⁴³ Furthermore, transmission electron microscope evaluation of mitochondria within neutrophils, skeletal muscle, semen epithelial cells and spermatozoa by Appleyard *et al.*⁴³, revealed that the mitochondria from affected dogs in all of the aforementioned tissues appeared reduced in size and number. Morphologically, the number of cristae within each mitochondrion appeared reduced and poor definition of the characteristic double cristal

membrane was noted.⁴³ These findings led to a hypothesis that a decreased energy supply to the retina and RPE may lead to retinal dysplasia in the Miniature Schnauzer dog.⁴³

As TFAM is known to control mitochondrial transcription activity and copy number⁴⁴, a mutation in the *Tfam* gene sequence of affected Miniature Schnauzer dogs could lead to the decreased retinal and RPE *Tfam* and mtDNA mRNA levels noted by Appleyard *et al.*⁴³ Therefore, the first objective of this study was to determine if the *Tfam* gene sequence is altered in Miniature Schnauzer dogs affected with retinal dysplasia and associated hyperplastic primary vitreous. Using the polymerase chain reaction (PCR), the coding sequence along with the promoter, intron1 and the 3'untranslated sequence to 218 bases beyond the polyadenylation site were amplified, cloned and sequenced for analysis. The second objective of this study was to objectively quantitate, measure the surface area, and compare the morphology of lymphocyte mitochondria from normal and affected Miniature Schnauzer dogs using transmission electron microscopy as well as compare mitochondrial morphology. The identification of *Tfam* sequence or mitochondrial differences would provide insight into the pathogenesis of retinal dysplasia and associated persistent hyperplastic primary vitreous in the Miniature Schnauzer dog.

1.2 MATERIALS AND METHODS

1.2.1 EXPERIMENT DESIGN

Experimental breeding of two known affected and two known unaffected Miniature Schnauzer dogs was performed. All eyes were examined by a veterinary ophthalmologist to verify whether the retina was normal or affected with the syndrome of retinal dysplasia and occasionally expressed PHPV. Normal dogs were also confirmed by test breeding and pedigree analysis. If phenotypically normal progeny were generated by an unknown and affected dog test breeding then the unknown dog genotype was confirmed to be normal. Physical examinations did not reveal any systemic abnormalities other than ocular defects. All animals were handled according to the standards set by the Canadian Council on Animal Care and the ARVO Statement for the Use of Animals and Ophthalmic and Vision Research.

1.2.2 SAMPLE PREPARATION AND DNA/RNA EXTRACTION

EDTA whole blood samples were collected by venipuncture from affected and unaffected subjects. The red blood cells were lysed with Tris ammonium chloride and the white blood cell pellets were collected via centrifugation. For electron microscopy, a portion of the white blood cells were fixed in 5% glutaraldehyde with 0.2 M s-collidine buffer. The cells were then embedded in Epon/Araldite, sectioned at a thickness of 90-100 nm, and stained with uranyl acetate. For PCR, the total cellular DNA of leukocytes was extracted by phenol/chloroform after treatment with proteinase K (Invitrogen™). The DNA was quantified using a spectrophotometer (Cary 100Bio) to measure the absorbance at 260 and 280 nm. For RNA isolation three 3-week old progeny from the experimental breeding were euthanized with an overdose of barbiturates and the retina and RPE were harvested from affected and unaffected eyes using an operating microscope in a sterile environment. The retinas from both eyes of each dog were removed from the posterior segment and placed into 10mL of extraction reagent (TRIzol; Invitrogen™). The posterior segment was then filled with approximately 1mL of 0.5% trypsin (Invitrogen™). After 5

minutes of incubation and gentle manipulation with a cyclodialysis spatula, the RPE cells from each eye were harvested. These cells were then pooled from both eyes and placed into 10mL of extraction reagent (TRIzol; Invitrogen™). cDNA was produced with reverse-transcription reactions primed with oligo-dT using the total harvested RNA as a template (5µg RNA per reaction).

1.2.3 PRIMER DESIGN

All *Tfam* gene data was obtained from GenBank® and based on the Boxer breed sequence assembled in May 2005 by the Broad Institute of MIT/Harvard. The *Tfam* gene (LOC488989) is made up of seven exons and lies within positions 13,787,958 to 13,801,337 of chromosome 4 (GenBank® accession number NC_006586). (Figure 1.1) The gene encodes the TFAM protein with a corresponding record of XP_546107. Optimal primers targeting the *Tfam* gene including intron1 and the 5' and 3' untranslated regions were designed using the program Primer Designer version 2.01 (Scientific and Educational Software) and synthesized by Invitrogen™. Primer design criteria included similarity in melting temperature (T_m) levels and avoidance of primer and template secondary structure at the primer T_m . A BLAST search of GenBank® was performed on the primers and the canine genome to ensure specificity. The nucleotide sequences and the properties of these primers are listed in Table 1.1.

1.2.4 PCR

Two different cycling protocols were necessary for *Tfam* amplification. For the promoter region (-253 to -9) and intron1 a 'Slowdown' protocol¹⁰⁸ with various annealing temperatures, prolonged cycles, and low ramp rates was used in an Eppendorf® Mastercycler® thermal cycler, as standard PCR was unsuccessful in these regions. From -115 to 218 bases beyond the polyadenylation site (Position +1621 bp) a standard PCR protocol was used in a Perkin Elmer 480 thermal cycler. For the untranslated regions (promoter, intron1 and 3' sequence) 5ng genomic DNA of affected or unaffected subjects was used as the template. Reactions for the translated regions were performed using

cDNA of affected or unaffected subjects as the template. PCR reactions were carried out in a total volume of 50 µl. Standard PCR contained buffer supplied by the manufacturer (United Bioinformatica Inc.: 50mmol/l KCl, 10mmol/l TrisHCl pH 8.8, 0.08% Nonidet-P40), 1.5 mmol/L MgCl₂, 200µmol/l each NTP, 1 U Taq Polymerase and 100 nmol/l of each primer. 'Slowdown' PCR used a standard PCR mixture except 150 µmol/l of 7-deaza-2'-deoxyguanosine-5'triphosphate dilithium salt (dc⁷GTP) (Amersham Biosciences) + 50 µmol/l GTP was used instead of 200 µmol/L GTP.

Standard PCR was performed for 30 cycles with 45 s denaturation at 94°C, 45 s annealing at 65 °C followed by a primer extension of 45 s at 72 °C. The 'Slowdown' protocol was used with a lowered ramp rate at 2.5°C/s and a low cooling rate for reaching annealing temperature at 1.5°C/s. The 'Slowdown' PCR was carried out under the following conditions: amplifications were run for 48 cycles with 30 s denaturation at 95°C, 30 s annealing with a progressively lowered temperature from 70°C to 55°C at a rate of 1°C every third cycle, and a primer extension of 40 s followed by 15 additional cycles with an annealing temperature of 58°C. Ten µl of PCR products were loaded on 2.5% agarose gels and visualized under UV-illumination. The PCR products of expected size were then ligated into a TOPO TA cloning vector (Invitrogen™) and used to transform competent *E. coli* DH5-α cells. Transformed colonies were identified by PCR and sequenced at the National Research Council Plant Biotechnology Institute (Saskatoon, Saskatchewan) using T7 primers. The cloned sequences of the affected and unaffected subjects were aligned with each other and with GenBank® using SeqAid II™ (Version 3.81) and base pair differences were examined. Nucleotide numbering was based on nucleotide +1 corresponding with the start of translation and intron nucleotides were numbered according to the number of the last nucleotide of the preceding exon followed by a plus sign and the nucleotide position in the intron.

1.2.5 ELECTRON MICROSCOPY

For mitochondrial evaluation, fixed white blood cells from eleven Miniature Schnauzer dogs were used: two affected male, two affected female, three normal male and four normal female dogs (ages 1-12 years). From each dog a minimum of 10 lymphocytes

were examined and photographed at 13, 000 magnification using a Philips EM 410 transmission electron microscope. Criteria for selecting lymphocytes were agranular cells with round or oval nuclei and little cytoplasm. Lymphocytes were the white blood cell of choice due to their ease of identification and the lack of cytoplasmic granules allowing for clear identification of mitochondria. Images were scanned into a computer and viewed using the Northern Eclipse (Empix Imaging Inc.) graphics program. Using the graphics program the perimeter of each lymphocyte photographed was measured in microns (μm) and the surface area (μm^2) was calculated. Mitochondria within each lymphocyte cross-section were identified and quantified. Selection criteria for the mitochondria included double membrane organelles with visible cristae. The perimeter of each mitochondrion was measured in microns (μm) and the mitochondrial surface area (μm^2) was calculated. (Figure 1.2) Lastly, using a masked observer, the scanned lymphocyte photographic images were viewed and the mitochondrial morphology was compared between affected and normal dogs.

1.2.6 STATISTICAL ANALYSIS

The median lymphocyte surface area, mitochondrial number per lymphocyte cross-section and mitochondrial surface area were compared between the affected and normal dogs. Since the distribution of the mitochondrial variables analyzed were non-Gaussian, comparisons were made using the non-parametric Mann-Whitney test. The lymphocyte surface areas were compared using a *t* test as the variables were parametric. A *p* value of <0.05 was accepted as significant. Statistical analysis was performed with GraphPad Software Inc. (San Diego, CA, USA).

1.3 RESULTS

1.3.1 *Tfam* SEQUENCING

Sequencing confirmed the PCR products obtained to be part of the *Tfam* gene. The cloned sequences of the affected and unaffected subjects were aligned with each other and with GenBank® accession number NC_006586 using SeqAid II™ (Version 3.81) and base pair differences were examined. No base pair changes of significance were noted. Base pair differences that were noted occurred between the GenBank® reference canine Boxer sequence (accession number NC_006586) and the affected and unaffected Miniature Schnauzers; not between the affected and unaffected dogs. Figures 1.3 to 1.5 demonstrate these differences. Nucleotide +1 corresponds with the start of translation and intron nucleotides were numbered according to the number of the last nucleotide of the preceding exon followed by a plus sign and the position in the intron. In the 5' non-coding promoter region at position -220 (position 13,788,128 on chromosome 4) the affected and unaffected Miniature Schnauzers differed from the GenBank® Boxer sequence in that both subjects had an adenosine versus a guanine recorded for the Boxer in GenBank® (Figure 1.3). Within the coding sequence no base pair changes were noted. Within intron1 the affected and unaffected dogs differed from GenBank® accession number NC_006586 in three positions. At Position 491+54 (position 13,788,502 on chromosome 4) the Miniature Schnauzers had a guanine versus GenBank® accession number NC_006586 had a thymine; at position 491+184 (position 13,788,632 on chromosome 4) a guanine versus a cytosine and at position 491+194 (position 13,788,642 on chromosome 4) a cytosine versus a guanine (Figure 1.4). After the STOP codon within the 3' non-coding sequence at position +1212 (position 13,801,179 on chromosome 4), GenBank® accession number NC_006586 was noted to have a cytosine and the affected and unaffected dogs were noted to have a thymine (Figure 1.5).

1.3.2 ELECTRON MICROSCOPY

A total of 151 lymphocytes were imaged and measured; 86 from normal dogs and 65 from affected dogs. Table 1.2 summarizes the overall results for each group. The normal dog lymphocyte surface area ranged from $7.94 \mu\text{m}^2$ to $31.74 \mu\text{m}^2$ with a median surface area of $20.04 \mu\text{m}^2$. The affected dog lymphocyte surface area ranged from $8.67 \mu\text{m}^2$ to $33.59 \mu\text{m}^2$ with a median surface area of $21.46 \mu\text{m}^2$. (Figure 1.6) The medians of lymphocyte surface area were not significantly different (p value = 0.3139). In the normal dog lymphocytes, mitochondrial numbers per cell cross-section ranged from zero to 10 with a median of 3.00. In the affected dog lymphocytes mitochondrial numbers per cell cross-section ranged from zero to 12 with a median of 2.00. (Figure 1.7) Using a Mann-Whitney test the medians were not statistically different ($p=0.8448$). The mitochondrial surface areas per lymphocyte cross-section were also compared. The normal dog mitochondrial surface area per lymphocyte cross-section ranged from $0.0196 \mu\text{m}^2$ to $0.7074 \mu\text{m}^2$ with a median of $0.1346 \mu\text{m}^2$. The affected dog mitochondrial surface area per lymphocyte cross-section ranged from $0.0187 \mu\text{m}^2$ to $0.4276 \mu\text{m}^2$ with a median of $0.1343 \mu\text{m}^2$. (Figure 1.8) No significant difference existed between the affected and normal mitochondrial surface areas per lymphocyte cross-section ($p=0.2047$). Lastly, mitochondrial morphology did not appear altered between the two groups.

1.4 DISCUSSION

The current study verified no significant base pair changes in the promoter region, coding sequence, intron1 or 3' non-coding sequence of the *Tfam* gene between affected and unaffected Miniature Schnauzer dogs. Similarly, there was no significant difference in mitochondrial number, size or morphology between affected and normal dogs. TFAM involvement in Miniature Schnauzers with retinal dysplasia was speculated recently by Appleyard *et al.*⁴³ As a gene's promoter region⁴⁵ and most commonly intron1⁴⁷⁻⁴⁹ can regulate gene transcription, mutations in these areas could lead to decreased gene transcription and thus decreased mRNA levels. Similarly, mutations in the *Tfam* gene coding and 3' non-coding sequence, including the polyadenylation site, could alter transcription efficiency resulting in decreased mRNA levels.^{53, 54} No evidence could be found in this study to support the hypotheses advanced by Appleyard *et al.*⁴³ concerning the pathogenesis of retinal dysplasia in the Miniature Schnauzer dog. The sequences of the *Tfam* gene examined are not altered in affected dogs with retinal dysplasia and the base pair changes noted between the Miniature Schnauzer dog and the GenBank® reference Boxer sequence (accession number NW_876311) (Figures 1.3 to 1.5) were assumed to be due to breed differences.

Various etiologies other than a mutation in the specific *Tfam* sequences analyzed could lead to the decreased retinal and RPE *Tfam* mRNA levels noted by Appleyard *et al.*⁴³ in the affected Miniature Schnauzer dog. *Tfam* gene expression is coordinated and regulated by highly specific transcription factors.^{67, 109-111} These factors are also known to regulate multiple nuclear genes whose products contribute to mitochondrial respiratory function.^{67, 110, 111} The promoter activity of the *Tfam* gene is highly dependent upon recognition sites for the transcription factors known as the nuclear respiratory factors 1 and 2 (NRF-1 and -2) and Sp1.¹⁰⁹ NRF-1 in particular has been demonstrated to provide a vital function during early embryonic development as an NRF-1 deficiency results in reduced mtDNA.¹¹² A more recent study confirmed recognition sites for the above transcription factors but also identified functional recognition sites for the transcription factor hStaf/ZNF143.¹¹¹ This study demonstrated that hStaf/ZNF143 is also necessary for obtaining efficient transcription levels from the *Tfam* promoter.¹¹¹ Lastly, another

transcription factor, Myc, has also been established to play a role in mitochondrial biogenesis through *Tfam* transcription regulation.¹¹³ *In situ*, Myc binds directly to the *Tfam* promoter region and contributes to *Tfam* expression.¹¹³

In addition to transcription factors, a transcriptional coactivator, peroxisome proliferator-activated receptor- γ coactivator-1 α (PGC-1 α) can induce mitochondrial biogenesis by interacting with NRF-1 on the *Tfam* promoter. PGC-1 α is markedly upregulated in brown fat during adaptive thermogenesis but is also expressed in various tissues not ordinarily associated with adaptive thermogenesis such as brain and heart. An increase in PGC-1 α expression has been demonstrated to lead to a significant increase in the expression of *Tfam* along with cellular mtDNA levels and mitochondrial mass in tissue-culture cells and in transgenic mice.¹¹⁴ A second coactivator, designated PGC-1-related-coactivator (PRC), is not significantly induced in adaptive thermogenesis but can also *trans* activate NRF-1 target genes that are necessary for the biogenesis of mitochondria and the expression of a functional respiratory chain.^{67, 114} With respect to Miniature Schnauzer dogs affected with retinal dysplasia, deficiencies or mutations in the aforementioned transcription factors and coactivators could result in the decreased *Tfam* mRNA levels reported by Appleyard *et al.*⁴³ Demonstrating the expression of these factors in retinal dysplasia may address the possibility of their involvement in this condition.

The inability of the aforementioned transcription factors and coactivators to bind to the *Tfam* promoter could also result in decreased *Tfam* expression. DNA methylation of CpG dinucleotides has been demonstrated to suppress the expression of many genes due to its direct interference with transcription factor binding.¹¹⁵ The *Tfam* promoter contains many CpG dinucleotides which are potential methylation sites and it has been demonstrated that *in vitro* methylation of the NRF-1 sites down-regulates *Tfam* expression.¹¹⁵ Thus, methylation of the *Tfam* promoter may silence *Tfam* expression and contribute to the decrease in mtDNA amount noted in an affected Miniature Schnauzer dog with retinal dysplasia. Examination of *Tfam* promoter methylation was not performed in this study.

Other factors affecting gene transcription in general could also cause the decreased *Tfam* mRNA noted by Appleyard *et al.*⁴³ The activities of many promoters are greatly

increased by sequences called enhancers that have no promoter activity of their own.⁴⁶ Enhancers can exert their stimulatory actions over distances of several thousand base pairs making them often difficult to identify. Various types of silencer elements can, however, block the activity of enhancers leading to suppression of transcription.¹¹⁶ Similarly, alternative promoters have been demonstrated to be situated in introns other than intron1.⁵⁰ Enhancers were not identified in this study and other introns were not amplified or sequenced.

A decreased level of *Tfam* mRNA can also result from transcript instability. The majority of eukaryotic mRNAs carry a 5' 7-methylguanosine cap structure and a 3' poly(A) tail that is bound to a poly(A) binding protein (PABP).¹¹⁷ Both of these structures protect the RNA chain from degradation by exonucleases.^{117, 118} Removal of the poly(A) tail from some stable mRNAs causes them to be degraded rapidly.¹¹⁹ Similarly, 5' decapping results in subsequent exonucleolytic mRNA degradation.¹¹⁷ Other reported factors affecting mRNA half-life include developmental or environmental stimuli such as nutrient levels, cytokines, hormones, temperature shifts and viral infection.¹¹⁷ Lastly, a decreased level of *Tfam* mRNA could also be due to down-regulation. If mtDNA amount is reduced in affected Miniature Schnauzer dogs through some other nuclear mechanism, decreased *Tfam* transcript level may simply reflect the decreased demand for TFAM.¹²⁰

Mammalian cells contain several hundreds to greater than a thousand mitochondria and the size, shape and abundance of mitochondria may change under different energy demands and different physiological or environmental conditions.¹²¹ It has been suggested that cells depleted of mtDNA have ultrastructurally abnormal mitochondria^{44, 122} and it has been demonstrated that TFAM-mutant mice with pancreatic cell disruption of TFAM have severe mtDNA depletion, deficient oxidative phosphorylation and abnormal appearing mitochondria.¹²³ In addition, a correlation between *Tfam* expression and content of mitochondria has also been demonstrated.¹²⁴ Based on these reports and the demonstration of decreased leukocyte mtDNA, decreased retinal and RPE *Tfam* mRNA and possibly decreased leukocyte mitochondrial numbers and size in affected Miniature Schnauzer dogs⁴³, further objective mitochondrial evaluation was warranted to determine if mitochondria play a role in Miniature Schnauzer dogs with retinal dysplasia. In this study, upon initial subjective evaluation of Miniature Schnauzer lymphocyte mitochondrial number and size,

there appeared to be a trend towards larger and more numerous mitochondria in the lymphocytes of normal Miniature Schnauzer dogs. However, after objective quantification there were no differences between the two groups. (Table 1.2) Using a masked technique, the morphology of the lymphocyte mitochondria also did not appear altered between the two groups. This is not unexpected as affected dogs are otherwise systemically healthy. Limitations of using transmission electron microscopy to evaluate mitochondria do exist. The classic measurement of mitochondrial section area by this method is limited by the complex three dimensional organization of mitochondria¹²⁵ and the internal organization of mitochondria is irregular and variable on physiological conditions.¹²⁶ A more accurate method of determining mitochondrial content is by measuring the citrate synthase activity.¹²⁴ Citrate synthase is localized within the mitochondrial matrix and its activity is commonly used as a quantitative enzyme marker for the presence of intact mitochondria.¹²⁴ If altered energy supply to the retina and RPE remains a proposed pathogenesis of retinal dysplasia in the Miniature Schnauzer dog, then evaluation of affected and normal retinal mitochondrial morphology and content by citrate synthase activity would be ideal.

Most importantly, the underlying question of whether *Tfam* mRNA is truly decreased in the retina and RPE of affected Miniature Schnauzer dogs needs to be answered. The original study by Appleyard *et al.*⁴³ used only one dog from each group when determining the relative quantity of *Tfam* mRNA. To base further research on this data, verification with increased samples would be necessary. This would be challenging as a repeat experimental breeding would be necessary to obtain retina and RPE tissue. mRNA expression has also been documented to be influenced by the stage of tissue development¹²⁷, thus, determining which genes are differentially expressed by the retina and RPE during the process of retinal dysplasia development in utero, would be ideal. Furthermore, although there is a tight connection between gene expression and gene product function¹²⁸, this is certainly not always the case. The study by Appleyard *et al.*⁴³ used real-time PCR to measure the mRNA levels of *Tfam* and several mitochondrial genes in the retina and RPE. These findings suggest possible decreases in TFAM and mitochondrial protein levels or function but formal demonstration or measurement of TFAM protein levels using Western blot analysis for example, would be necessary to confirm a role of TFAM in affected Miniature Schnauzer dogs with retinal dysplasia.

In conclusion, this study demonstrated that the *Tfam* promoter, intron1, coding and 3'non-coding sequence is not altered in Miniature Schnauzer dogs affected with retinal dysplasia. Furthermore, there is no significant difference in lymphocyte mitochondrial number, surface area or morphology between affected and normal dogs. Further investigations into other candidate genes causing retinal dysplasia in the Miniature Schnauzer dog are warranted.

Table 1.1 Oligonucleotide sequences of *TFam* primers with calculated T_m and GC content.

Primer	Sequence	T_m (°C)	Pos	Product Length	GC cont. (%)
TFAM 138s	5'-CCG AGC TCC TCC TCC TTT GC-3'	60.3	-253 bp	245 bp	65.0
TFAM 363as	5'-CCT ACA ACG CAG CGA CCG AG-3'	60.6	-28 bp		65.0
TFAM 138s	5'-CCG AGC TCC TCC TCC TTT GC-3'	60.3	-253 bp	580 bp	65.0
TFAM 698as	5'-TGC CTG CCA GTC TGC CCT AT-3'	65.4	+30 bp		60.0
TFAM 535s	5'-TAC CCA AAG AAG CCT CTG AC-3'	57.0	+145 bp	573 bp	50.0
TFAM 1088as	5'-TCC TTG GTG CTT TAC TGA GC-3'	58.1	+698 bp		50.0
TFAM 704s	5'-CAG ACT GGC AGG CAT ACA AAG-3'	60.8	+314 bp	889 bp	52.4
TFAM 1573as	5'-AGA GGA GTT GTG GGT GCT CT-3'	58.9	+1183 bp		55.0
TFAM 1081s	5'-CTA CGT CGC TCA GTA AAG CAC-3'	60.0	+691 bp	950 bp	55.0
TFAM 2011as	5'-CTG GCT GTG CCT TGT TAT GGA-3'	62.2	+1621 bp		55.0
TFAM 367s	5'-GTC GCT GCG TTG TAG GCT GG-3'	66.5	-24 bp	716 bp	65.0
TFAM 1063ias	5'-GTC AGA GGC TTC TTT GGG TA-3'	57.0	+145 bp		50.0

Primer position was calculated relative to translation start point.

Table 1.2 Lymphocyte surface area and mitochondrial quantification and surface area measurement using electron microscopy of normal and affected Miniature Schnauzer dogs at 13,000 X magnification.

	Total # of Lymphocytes	Median Lymphocyte Surface Area (μm^2)	Median Mitochondrial #/Lymphocyte Cross- section	Median Mitochondrial Surface Area (μm^2)/Lymphocyte Cross-section
Affected	86	21.46	2	0.1343
Unaffected	65	20.04	3	0.1346

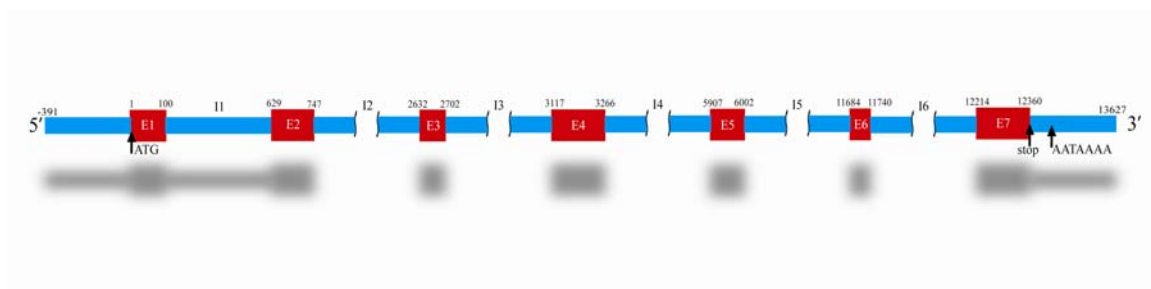


Figure 1.1. TFAM gene structure. Numbering is relative to the start codon. The areas sequenced are shadowed. I = intron, E = exon.

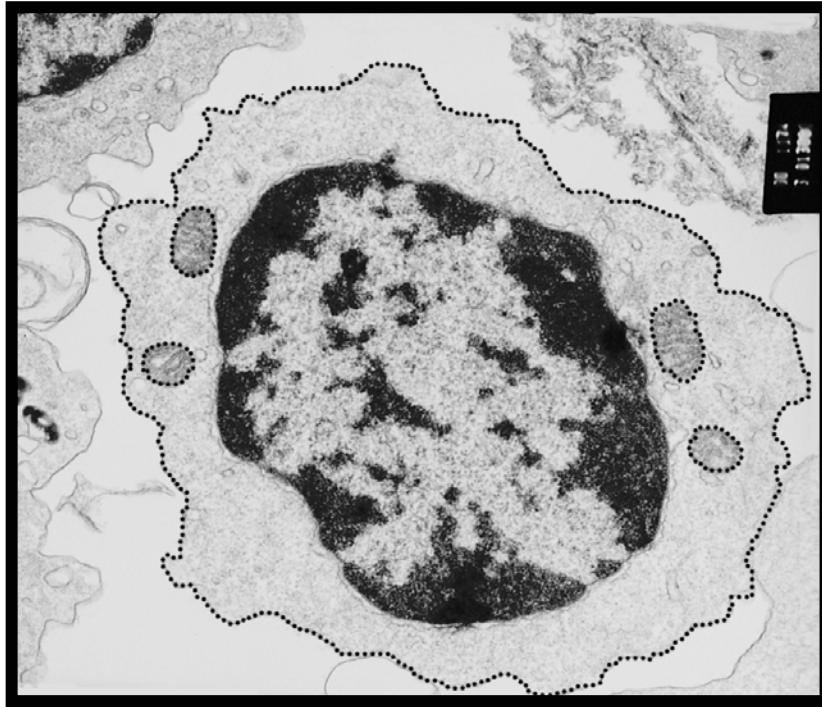


Figure 1.2 Transmission electron micrograph of a canine lymphocyte. The cell and mitochondria are outlined for surface area measurement. Magnification x 13,000.

		-240		*		-220		*		-200
Affected	:	CTCCTCCTTTGCAGCCCCGCCCACCAAGGAAAGCCGCTACGACGCCT								
Unaffected	:	CTCCTCCTTTGCAGCCCCGCCCACCAAGGAAAGCCGCTACGACGCCT								
NC_006586	:	CTCCTCCTTTGCAGCCCCGCCCACCAAGGAAAGCCGCTACGACGCCT								

Figure 1.3 Alignment of the partial *Tfam* sequences from affected and normal Miniature Schnauzer promoter region compared to the GenBank® Boxer canine sequence (derived from accession number NC_006586). Region with variation is shaded in grey. Numbering corresponds with the nucleotide position relative to the start of translation.

		40		*		60		*	
Affected	:	GCGCGCCCAGGACGCCCTGGGGTTGGAGTGTGTACTTTTTGCCCCCT							
Unaffected	:	GCGCGCCCAGGACGCCCTGGGGTTGGAGTGTGTACTTTTTGCCCCCT							
NC_006586	:	GCGCGCCCAGGACGCCCTGGGGTTGGAGTGTGTACTTTTTGCCCCCT							

		180		*		200		*	
Affected	:	CACCGTCCCCCGCCTCCTCCCGCCCCACCGCACTGTCCAACCTT							
Unaffected	:	CACCGTCCCCCGCCTCCTCCCGCCCCACCGCACTGTCCAACCTT							
NC_006586	:	CACCGTCCCCCGCCTCCTCCCGCCCCACCGCACTGTCCAACCTT							

Figure 1.4 Alignment of the partial *Tfam* sequences of intron1 from affected and normal Miniature Schnauzer compared to the GenBank® Boxer canine sequence (derived from accession number NC_006586). Regions with variation are shaded in grey. Numbering corresponds with the nucleotide position within intron1.

	1200	*	1220
Affected	: ACTCCTCTAGGTAAATT	T	CAATTTCTAGGTA
Unaffected	: ACTCCTCTAGGTAAATT	T	CAATTTCTAGGTA
NC_006586	: ACTCCTCTAGGTAAATT	C	CAATTTCTAGGTA

Figure 1.5 Alignment of the partial *Tfam* sequences of the 3' non-coding region from affected and normal Miniature Schnauzer compared to the GenBank® Boxer canine sequence (derived from accession number NC_006586). Region with variation is shaded in grey. Numbering corresponds with the nucleotide position relative to the start of translation.

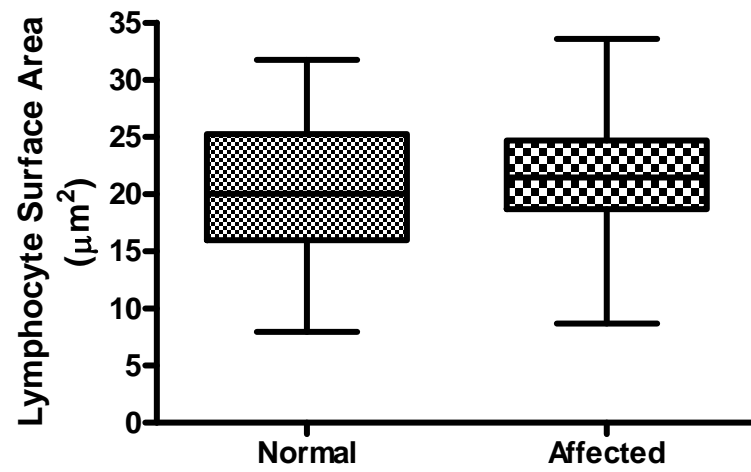


Figure 1.6 Box and whisker graphs of lymphocyte surface area of normal and affected Miniature Schnauzer dogs.

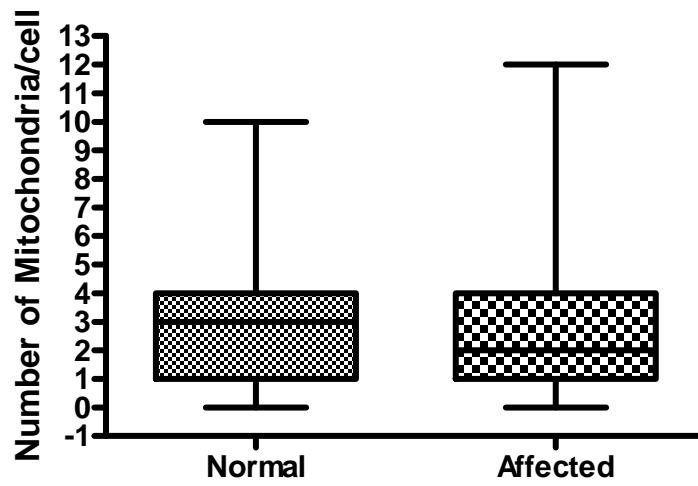


Figure 1.7 Box and whisker graphs of mitochondrial numbers per lymphocyte cross-section of normal and affected Miniature Schnauzer dogs.

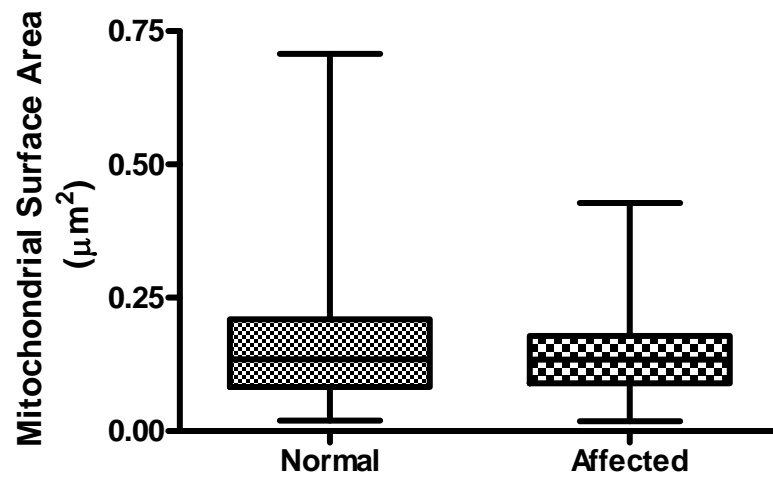


Figure 1.8 Box and whisker graphs of mitochondrial surface area per lymphocyte cross-section of normal and affected Miniature Schnauzer dogs.

CHAPTER 2

RELATIVE QUANTITATION OF LEUKOCYTE MITOCHONDRIAL DNA AND MITOCHONDRIAL EVALUATION USING TRANSMISSION ELECTRON MICROSCOPY IN NORMAL ENGLISH SPRINGER SPANIEL DOGS AND THOSE AFFECTED WITH RETINAL DYSPLASIA

2.1 INTRODUCTION

Inherited retinal dysplasia has been well studied in the English Springer Spaniel dog, yet the pathogenesis remains unknown. Fetal English Springer Spaniel eyes with retinal dysplasia have been noted via light and electron microscopy to have a marked decrease in the size and area occupied by the gap junctions within the external limiting membrane compared to normal fetuses.⁹⁴ It has therefore been proposed that inappropriate expression of cell adhesion molecules or glycoproteins on the neuroepithelium or Müller cells may lead to poor cell adhesion. This in turn may lead to the inability to form cell junctions or proper cell-cell communication, causing subsequent disorganized proliferation of neuroblasts and the typical retinal dysplasia rosettes noted with light microscopy.¹ Further studies by Whiteley *et al.*¹⁰¹ demonstrated differences in intramembranous particle density and filipin binding in affected English Springer Spaniel dogs compared to age-matched controls, suggesting that abnormalities in the membrane structure of neuroblastic cells may be related to the dysplastic process.¹⁰¹ O'Toole *et al.*²⁰ have proposed that defective development of Müller cells or abnormal gliovascular relationships may result in retinal dysplasia, as disorganized Müller fibres within the dysplastic areas and the focal absence of a discrete external limiting membrane have been noted histologically.²⁰ These mechanisms may also explain other aspects of this disease, including retinal detachment and persistence of the hyaloid vasculature.^{20, 98}

The most recent study investigating the pathogenesis of retinal dysplasia in the dog was by Appleyard *et al.*⁴³ Using real-time PCR in the Miniature Schnauzer dog Appleyard *et al.*⁴³ revealed that the white blood cells of an affected dog with retinal

dysplasia had decreased mitochondrial DNA (mtDNA) compared to a normal Miniature Schnauzer dog.⁴³ Further investigations in this study demonstrated that the retina and RPE of the affected Miniature Schnauzer dog had decreased expression of several mitochondrial genes as well as *Tfam*⁴³, a nuclear encoded gene controlling mitochondrial transcription and copy number.⁴⁴ These findings led to the postulation that retinal dysplasia in this breed may be due to decreased retinal energy supply.⁴³ Using transmission electron microscopy, Appleyard *et al.*⁴³ also believed that the mitochondria of affected Miniature Schnauzer dogs were decreased in numbers and size and appeared to have altered morphology.⁴³

Ophthalmoscopically and histologically, retinal dysplasia in the English Springer Spaniel dog is similar to that in the Miniature Schnauzer dog. In both breeds, retinal dysplasia is inherited as a bilateral, generalized condition. Histologically, affected individuals of both breeds have been demonstrated to have an incomplete external limiting membrane, convoluted outer nuclear layer, and dysplastic outer and inner segments.^{15, 20} Due to the similarities of the condition in both breeds, the molecular and morphological findings of Appleyard *et al.*⁴³ may not be unique to the Miniature Schnauzer dog. One objective of this study was to compare the relative amounts of mtDNA in the white blood cells of several normal and affected English Springer Spaniel dogs using real-time PCR. Identifying decreased mtDNA in the white blood cells of affected dogs could provide a potential screening test for identifying the condition. Secondly, quantification, measurement and morphology assessment of lymphocyte mitochondria was performed. Identifying significant differences between the two groups could provide further insight into identifying the pathogenesis of retinal dysplasia in the English Springer Spaniel dog.

2.2 MATERIALS AND METHODS

2.2.1 EXPERIMENT DESIGN

For mtDNA relative quantification seven affected and five unaffected English Springer Spaniel dogs ranging in age from 1 to 11 years were selected. For mitochondrial evaluation, seven English Springer Spaniel dogs were used: two affected male, one affected female and four normal female dogs (ages 1-11 years). All eyes were examined by a veterinary ophthalmologist to verify whether the retina was normal or affected with retinal dysplasia. General physical examinations did not reveal any systemic abnormalities other than ocular defects. All animals were handled according to the standards set by the Canadian Council on Animal Care and the ARVO Statement for the Use of Animals and Ophthalmic and Vision Research.

2.2.2 SAMPLE PREPARATION AND DNA EXTRACTION

EDTA whole blood samples were collected by venipuncture from affected and unaffected subjects. The red blood cells were lysed with Tris ammonium chloride and the white blood cell pellets were collected via centrifugation. For electron microscopy, a portion of the white blood cells were fixed in 5% glutaraldehyde with 0.2 M s-collidine buffer. The cells were then embedded in Epon/Araldite, sectioned at a thickness of 90-100nm and stained with uranyl acetate. For PCR, the total cellular DNA of leukocytes was extracted by phenol/chloroform after treatment with proteinase K (Invitrogen™). The DNA was quantified using a spectrophotometer (Cary 100Bio) to measure the absorbance at 260 and 280 nm.

2.2.3 PRIMER DESIGN AND PCR CONDITIONS

Using cytochrome oxidase subunit 1 (COX-1) as a representative of mtDNA and glyceraldehyde-3-phosphate dehydrogenase (GA-3-PDH) as a reference gene to normalize COX-1 levels, the relative quantitation of COX-1 between normal dogs and then normal

against affected dogs was performed using a Mx 3005P Stratagene Multiplex Quantitative PCR System. Optimal primers for COX-1 and GA-3-PDH were designed using the program Primer Designer version 2.01 (Scientific and Educational Software) and synthesized by Invitrogen™. Primer design criteria included similarity in melting temperature (T_m) levels and avoidance of primer and template secondary structure at the primer T_m . A BLAST search of Genbank® was performed on the primers and the canine genome to ensure specificity. The designed primer pairs were tested in a standard PCR reaction and visualized with ethidium bromide after agarose gel electrophoresis. Those primers producing a clean, single product of expected size were selected and further tested for their ability to produce a sharp melting curve peak after successive PCR cycles in a thermal cycler (Mx 3005P Stratagene). The nucleotide sequences of the primer pairs selected are:

GA-3-PDH: sense (S) 256 5'-GGTGATGCTGGTGCTGAGTAT $T_m = 59.6^\circ\text{C}$ and antisense (AS) 439 5'-TGCTGACAATCTTGAGGGAGT $T_m = 59.3^\circ\text{C}$, yielding a 183 bp product with a calculated T_m of 91.8°C and a measured T_m of 86.5°C .

COX-1: S 893 5'-GATGTAGACACACGAGCGTA $T_m = 55^\circ\text{C}$ and AS 970 5'-CCATGAAGTGTTGCCAGT $T_m = 55^\circ\text{C}$, yielding a 77bp product, with a calculated T_m of 82.4°C and a measured T_m of 80.3°C .

PCR amplifications were carried out in a total volume of 25 μl , containing 0.5 μM of each primer, 12.5 μl of Brilliant® SYBR® Green QPR master mix (Stratagene®), 0.375 μl of 1:500 diluted reference dye and 20ng of DNA. The PCR cycling conditions were: initial denaturation at 94°C for 30 seconds followed by an annealing temperature of 60°C for 45 seconds and an extension temperature of 72°C for 45 seconds. PCR amplification was performed in quadruplicate for each DNA sample and each experiment was repeated once. The SYBR® Green fluorescence intensities during PCR were recorded and analyzed in the MX 3005P system (Stratagene®). PCR amplification efficiencies for COX-1 and GA-3-PDH were calculated using data from a standard curve. The threshold cycle (C_T) is defined as the cycle at which the first significant increase in the fluorescent signal is detected. C_T values of the target gene (COX-1) were normalized to the reference gene (GA-3-PDH) and the relative quantification was performed according to the delta-delta C_T ($\Delta\Delta C_T$) model¹⁰⁵ and the Pfaffl model¹⁰⁶.

2.2.4. MELTING CURVE ANALYSIS

The melting curve analysis to ensure product homogeneity is provided by the system software and was performed after the real-time PCR. The amplified products were incubated at 95°C for 1 minute followed by ramped up temperatures of 55°C to 95°C at a rate of 0.2°C/sec with the fluorescence data being collected continuously on the 55-95°C ramp.

2.2.5 ELECTRON MICROSCOPY

From each dog a minimum of 10 lymphocytes were examined and photographed at 13, 000 magnification using a Philips EM 410 transmission electron microscope. Criteria for selecting lymphocytes were agranular cells with round or oval nuclei and little cytoplasm. Lymphocytes were the white blood cell of choice due to their ease of identification and the lack of cytoplasmic granules allowing for clear identification of mitochondria. Images were scanned into a computer and viewed using the Northern Eclipse (Empix Imaging Inc.) graphics program. Using the graphics program the perimeter of each lymphocyte photographed was measured in microns (μm) and the surface area (μm^2) was calculated. Mitochondria within each cell cross-section were identified and quantified. Selection criteria for the mitochondria included double membrane organelles with visible cristae. The perimeter of each mitochondrion was measured in microns (μm) and the mitochondrial surface area (μm^2) per lymphocyte cross-section was calculated. (Figure 2.1) Lastly, using a masked observer, the scanned lymphocyte photographic images were viewed and the mitochondrial morphology was compared between affected and normal dogs.

2.2.6 STATISTICAL ANALYSIS

The median lymphocyte surface area, mitochondrial number per lymphocyte cross-section and mitochondrial surface area were compared between the affected and normal dogs. Since the distribution of the mitochondrial variables analyzed were non-Gaussian,

comparisons were made using the non-parametric Mann-Whitney test. The lymphocyte surface areas were compared using a t test as the variables were parametric. A p value of <0.05 was accepted as significant. Statistical analysis was performed with GraphPad Software Inc. (San Diego, CA, USA).

2.3 RESULTS

2.3.1 REAL TIME PCR

The amplification efficiencies for GA-3-PDH and COX-1 were 1.883 and 1.913 respectively. (See Figures 2.2 and 2.3) For normal English Springer Spaniel dogs the C_T values for GA-3-PDH and COX-1 are provided in Table 2.1. The normalized ΔC_T and $\Delta\Delta C_T$ values calibrated to Dog 1 along with the relative ratios using the $\Delta\Delta C_T$ method¹⁰⁵ are also provided in Table 2.1. Using COX-1 as the target gene representative of mtDNA, the amount of mtDNA in unaffected dogs relative to unaffected Dog 1 is shown in Figure 2.4. Results revealed that the mtDNA amount was variable in normal English Springer Spaniel dogs and ranged from 1.08-fold difference to 4.76-fold difference. Dog 1 appeared to have the least amount of mtDNA. As affected dogs were hypothesized to have less mtDNA versus normal, mtDNA amount of the affected dogs was calibrated against Dog 1. C_T values along with ΔC_T and $\Delta\Delta C_T$ values for Dog 1 and the affected dogs are shown in Table 2.2. When comparing the affected dogs to a normal dog (Dog 1) with the lowest mtDNA amount the relative quantities ranged from a 1-fold to 2.68-fold difference. (See Figure 2.5) The relative ratios obtained by the Pfaffl model¹⁰⁶, which corrects for differences in amplification efficiency, were similar to those values obtained by the $\Delta\Delta C_T$ method¹⁰⁵ (results not shown). Homogeneity of the accumulated PCR products was confirmed in the assays by dissociation curves which show single sharp peaks. (Figure 2.6)

2.3.2 ELECTRON MICROSCOPY

A total of 81 lymphocytes were imaged and measured; 48 from normal dogs and 33 from affected dogs. Table 3 summarizes the overall results for each group. The normal dog lymphocyte surface area ranged from $8.76\mu\text{m}^2$ to $28.56\mu\text{m}^2$ with a median surface area of $17.62\mu\text{m}^2$. The affected dog lymphocyte surface area ranged from $8.79\mu\text{m}^2$ to $26.48\mu\text{m}^2$ with a median surface area of $18.94\mu\text{m}^2$. (Figure 2.7) Using a t test the means of lymphocyte surface area were not significantly different (p value = 0.0967). In the normal

dog lymphocytes, mitochondrial numbers per cell cross-section ranged from zero to 9 with a median of 3. In the affected dog lymphocytes mitochondrial numbers per cell cross-section ranged from zero to 12 with a median of 3. (Figure 2.8) Using a Mann-Whitney test the medians were not statistically different ($p=0.8098$). The mitochondrial surface areas per lymphocyte cross-section were also compared. The normal dog mitochondrial surface area per lymphocyte cross-section ranged from $0.0199 \mu\text{m}^2$ to $0.3090 \mu\text{m}^2$ with a median of $0.0912 \mu\text{m}^2$. The affected dog mitochondrial surface area per lymphocyte cross-section ranged from $0.0209 \mu\text{m}^2$ to $0.3420 \mu\text{m}^2$ with a median of $0.0954 \mu\text{m}^2$. (Figure 2.9) Statistical analysis with the Mann-Whitney test showed no significant difference between the affected and normal dog mitochondrial surface areas per lymphocyte cross-section ($p=0.3102$). Lastly, mitochondrial morphology did not appear altered between the two groups.

2.4 DISCUSSION

The results of this study indicate that the mtDNA amount in the white blood cells of affected and unaffected English Springer Spaniel dogs varies widely and is independent of whether dogs are affected with retinal dysplasia or not. Additionally, using transmission electron microscopy, there were no significant differences in lymphocyte mitochondrial number, size or morphology between affected and normal English Springer Spaniel dogs. It was recently suggested that the pathogenesis of retinal dysplasia in Miniature Schnauzer dogs may arise from a lowered energy supply to the retina and RPE.⁴³ This proposed pathogenesis was from data revealing decreased white blood cell mitochondrial DNA (mtDNA) in an affected Miniature Schnauzer dog and decreased mitochondrial number and size in multiple tissues of affected Miniature Schnauzer dogs.⁴³ In the following experiment, the relative quantity of leukocyte mtDNA in multiple affected and unaffected English Springer Spaniel dogs were compared within real-time PCR experiments. Using only normal dogs in one real-time experiment (Figure 2.4) the variation ranged from 1.08-fold to 4.76-fold difference. As affected dogs were hypothesized to have less mtDNA versus normal, mtDNA amount of the affected dogs were calibrated against Dog 1. Comparing affected dogs against a normal dog with the lowest amount of mtDNA (Dog 1) showed significant variation. The affected dogs had either a similar amount of mtDNA or up to 2.66-fold more. (Figure 2.5) The comparison of affected dogs to Dog1 only (versus the using the average of the normal dogs) was the most robust method to avoid a false claim. The calculated relative ratios of mtDNA were similar when both the $\Delta\Delta C_T$ method¹⁰⁵ and the Pfaffl method¹⁰⁶ were used indicating that the difference in amplification efficiencies of GA-3-PDH and COX -1 (1.883 and 1.913 respectively) played an insignificant role in relative quantitation.

Mitochondrial biogenesis and mtDNA maintenance depend on coordinated expression of genes in the nucleus and the mitochondria. The abundance of mitochondria and mtDNA necessary to meet a cell's energy needs is determined by a variety of hormonal and second messenger signals and may change under different energy demand and physiological or environmental conditions.¹²¹ Thus, a variety of factors can influence the amount of mtDNA in a particular cell. It has been proposed that increased oxidative

stress contributes to the abundance of mitochondria as well mtDNA content.¹²¹ This has been demonstrated in the leukocyte where elevated oxidative stress leads to increased mtDNA amounts.¹²⁹ Additionally, hyperlipidemia has been demonstrated to result in decreased mtDNA.¹³⁰ The blood samples from the English Springer Spaniel dogs used in this study were not grossly lipemic but exact measurements of lipoproteins were not measured.

The effect of age on mtDNA amount is controversial and tissue dependent.¹³¹ In many tissues (heart¹³², lung¹³³, kidney¹³², and spleen¹³²) mtDNA content has been demonstrated to increase with age whereas tissues such as the bone marrow show no age-related pattern.¹³² Demonstrations of mtDNA content in relation to age in the brain^{132, 134} and skeletal muscle^{120, 132, 135-137} are inconsistent. To the author's knowledge, the correlation of mtDNA and age within the white blood cell has not been investigated. In this particular study the age of the animal did not appear to correlate with leukocyte mtDNA content. However, based on the literature from other tissues, age matched controls should be performed if mtDNA content is to be further evaluated in dogs affected with retinal dysplasia. Lastly, previous studies have indicated that mtDNA concentrations are only weakly related to age-adjusted aerobic fitness (maximal oxygen consumption and self-reported physical activity levels)¹³⁶ and thus aerobic fitness of each dog was not considered to play a significant role in this particular study.

The question of whether mtDNA is truly decreased in the white blood cells of all affected Miniature Schnauzer dogs still, however, remains to be answered. The original study by Appleyard *et al.*⁴³ used only one dog from each group when determining the relative quantity of mtDNA. To base further research on this data, verification with increased samples would be necessary. Additionally, mtDNA content varies widely in different tissues¹³² with the differences observed being likely secondary to tissue-specific energy demands.¹²⁴ Therefore, as dogs affected with retinal dysplasia are otherwise healthy, the relative quantitation of mtDNA in the retina and RPE of age-matched affected and normal dogs rather than leukocytes, would be ideal to prove that decreased mtDNA is involved in the pathogenesis of the condition. It must also be noted, however, that although the original study by Appleyard *et al.*⁴³, demonstrated decreased retinal and RPE mitochondrial transcripts in the affected Miniature Schnauzer dog, mtDNA content and

transcript level do not always have a positive correlation.¹³⁴ In the brain, it has been demonstrated that aging has been associated with increased mtDNA content and reduced transcript level.¹³⁴ Similarly, in liver, heart, and skeletal muscle, a decline in mtDNA does not correlate with a decrease in transcript level nor do reduced mtDNA levels appear to affect enzyme activities.¹³¹ To the author's knowledge, other than the findings by Appleyard *et al.*⁴³, the correlation between mtDNA content and transcript level have not been evaluated in healthy retina and RPE.

Mitochondrial DNA depletion in association with abnormal mitochondria has been reported in several studies.^{43, 44, 123} Pancreatic cells with severe mitochondrial depletion and deficient oxidative phosphorylation have been noted to have abnormal mitochondria^{123, 138}, as well as mtDNA depleted myoblasts and mice embryos.^{44, 138} The recent study demonstrating a relative decrease in mtDNA in a Miniature Schnauzer dog affected with retinal dysplasia along with a possible decrease in leukocyte mitochondrial number and size as well as altered mitochondrial morphology⁴³, led to mitochondrial quantification and measurement in the English Springer Spaniel dog. Objective quantification and measurement of lymphocyte mitochondria in the English Springer Spaniel dog demonstrated no differences in mitochondrial number, size or morphology between normal dogs and those affected with retinal dysplasia. (Table 2.3) These results were not unexpected as affected dogs are otherwise systemically healthy. The demonstration in this study that leukocyte mtDNA is not decreased in affected versus normal English Springer Spaniel dogs also supports these electron microscopic findings. Limitations of using transmission electron microscopy to evaluate mitochondria do, however, exist. The classic measurement of mitochondrial section area by this method is limited by the complex three dimensional organization of mitochondria¹²⁵ and a more accurate method of determining mitochondrial content would be by measuring the citrate synthase activity.¹²⁴ Furthermore, if altered energy supply to the retina and RPE remains as a proposed pathogenesis of retinal dysplasia then objective evaluation of affected and normal retinal mitochondria would be ideal.

In conclusion, in contrast to the findings in the Miniature Schnauzer dog by Appleyard *et al.*⁴³, a relative decrease in white blood cell mtDNA does not exist in English Springer Spaniel dogs affected with retinal dysplasia. Furthermore, affected English

Springer Spaniel dog lymphocytes do not have decreased mitochondrial number, surface area or altered morphology when compared to normal English Springer Spaniel dogs. The essential question of whether decreased mtDNA is a feature of affected Miniature Schnauzer dogs remains to be answered, as the original study by Appleyard *et al.*⁴³ lacks power due to its low sample number. Evaluation of mitochondria, mtDNA and mitochondrial gene expression within age-matched retina and RPE of English Springer Spaniels would be necessary to determine if mitochondria play a role in the pathogenesis of retinal dysplasia in this breed.

Table 2.1 Comparison of differences in mean crossing threshold (C_T) \pm the standard deviation (S.D.) for COX-1 and GA-3-PDH for unaffected English Springer Spaniel dogs. Values are normalized (ΔC_T) and calibrated ($\Delta\Delta C_T$) to Dog 1. R = relative fold difference.

Unaffected	Dog 1	Dog 2	Dog 3	Dog 4	Dog 5
C_T COX-1	19.46 ± 0.13	19.69 ± 0.10	17.86 ± 0.10	21.83 ± 0.16	20.35 ± 0.10
C_T GA-3-PDH	15.55 ± 0.05	15.89 ± 0.05	16.20 ± 0.04	18.50 ± 0.19	18.03 ± 0.10
ΔC_T	3.91 ± 0.14	3.8 ± 0.11	1.66 ± 0.11	3.33 ± 0.25	2.32 ± 0.14
$\Delta\Delta C_T$	0.00 ± 0.14	-0.11 ± 0.11	-2.25 ± 0.11	-0.58 ± 0.25	-1.59 ± 0.14
R	1.00	1.08	4.76	1.49	3.01

Table 2.2 Comparison of differences in mean crossing threshold (C_T) \pm the standard deviation (S.D.) for COX-1 and GA-3-PDH for affected English Springer Spaniel dogs. Values are normalized (ΔC_T) and calibrated ($\Delta\Delta C_T$) to Dog 1.

	Dog 1	Dog 6	Dog 7	Dog 8	Dog 9	Dog 10	Dog 11	Dog 12
C_T COX-1	17.70 ± 0.03	22.79 ± 0.13	19.82 ± 0.08	20.02 ± 0.22	19.36 ± 0.13	17.55 ± 0.09	16.63 ± 0.11	17.94 ± 0.05
C_T GA-3-PDH	16.39 ± 0.06	22.89 ± 0.07	18.90 ± 0.07	18.66 ± 0.12	18.85 ± 0.07	16.51 ± 0.16	15.69 ± 0.09	17.92 ± 0.04
ΔC_T	1.31 ± 0.06	-0.1 ± 0.15	0.92 ± 0.11	1.36 ± 0.25	0.51 ± 0.15	1.04 ± 0.18	0.94 ± 0.14	0.02 ± 0.06
$\Delta\Delta C_T$	0.00 ± 0.06	-1.41 ± 0.15	-0.39 ± 0.11	0.05 ± 0.25	-0.8 ± 0.15	-0.27 ± 0.18	-0.37 ± 0.14	-1.29 ± 0.06
R	1.00	2.66	1.31	1.04	1.74	1.21	1.29	2.45

Table 2.3 Lymphocyte surface area and mitochondrial quantification and surface area measurement using electron microscopy of normal and affected English Springer Spaniel dogs at 13,000 magnification.

	Total # of Lymphocytes	Median Lymphocyte Surface Area (μm^2)	Median Mitochondrial #/lymphocyte cross section	Median Mitochondrial Surface Area (μm^2)
Affected	33	18.94	3	0.0954
Unaffected	48	17.62	3	0.0912

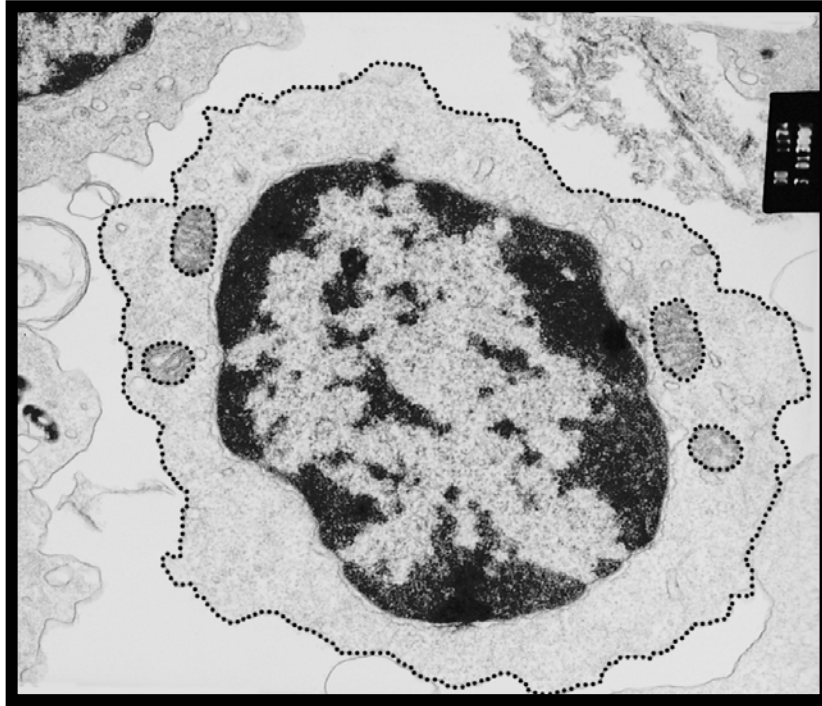


Figure 2.1 Transmission electron micrograph of a canine lymphocyte. The cell and mitochondria are outlined for surface area measurement. Magnification x 13,000.

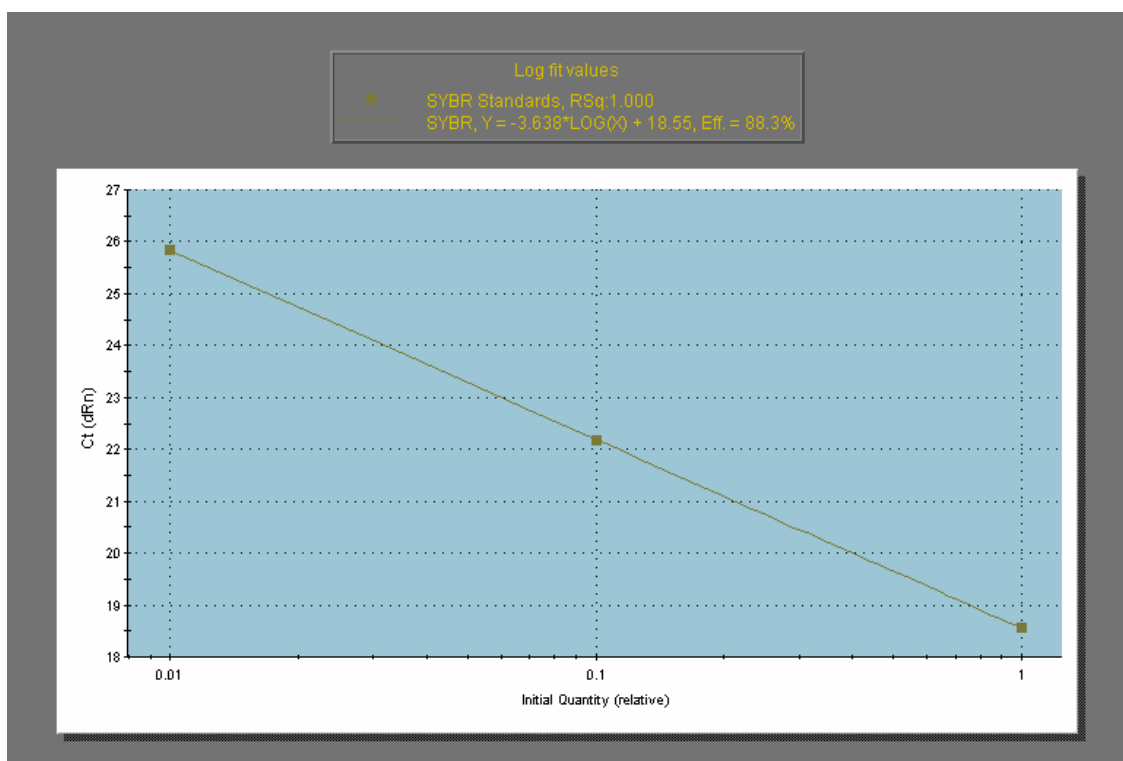


Figure 2.2 Standard curve for GA-3-PDH demonstrating a calculated efficiency of 1.883.

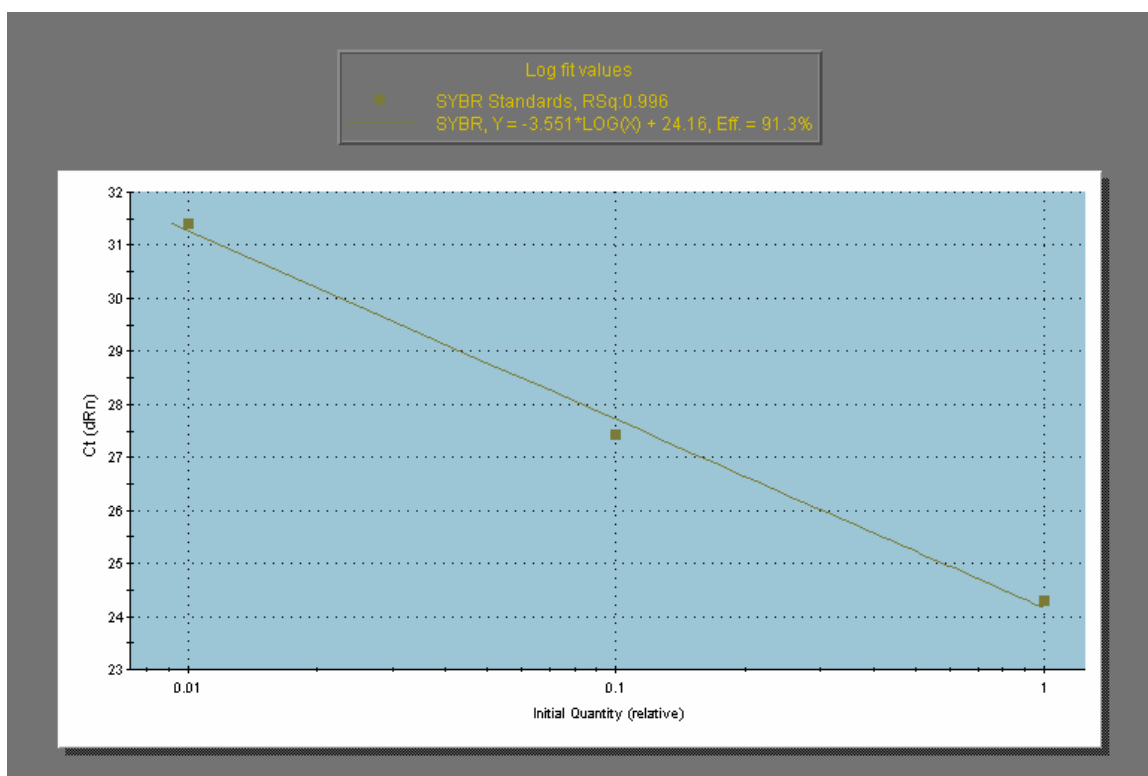


Figure 2.3 Standard curve for COX-1 demonstrating a calculated efficiency of 1.913.

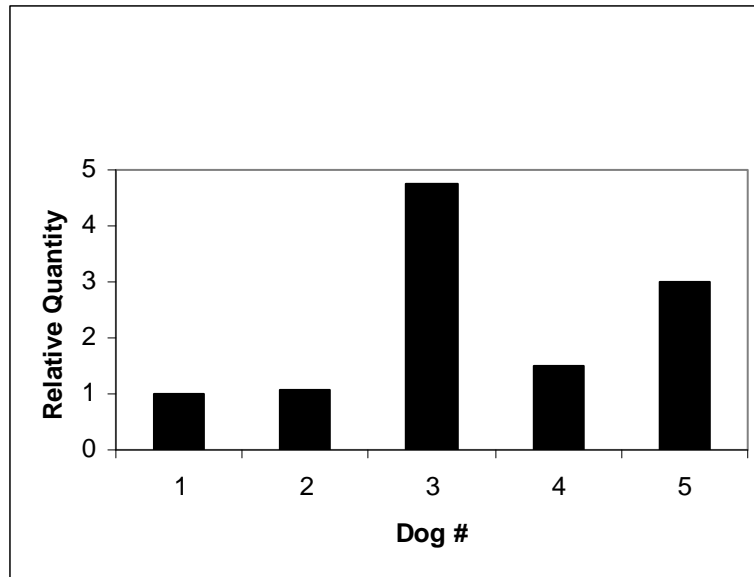


Figure 2.4 Relative amount of leukocyte mtDNA from normal English Springer Spaniel dogs. The results are expressed as a ratio relative to the value for Dog 1.

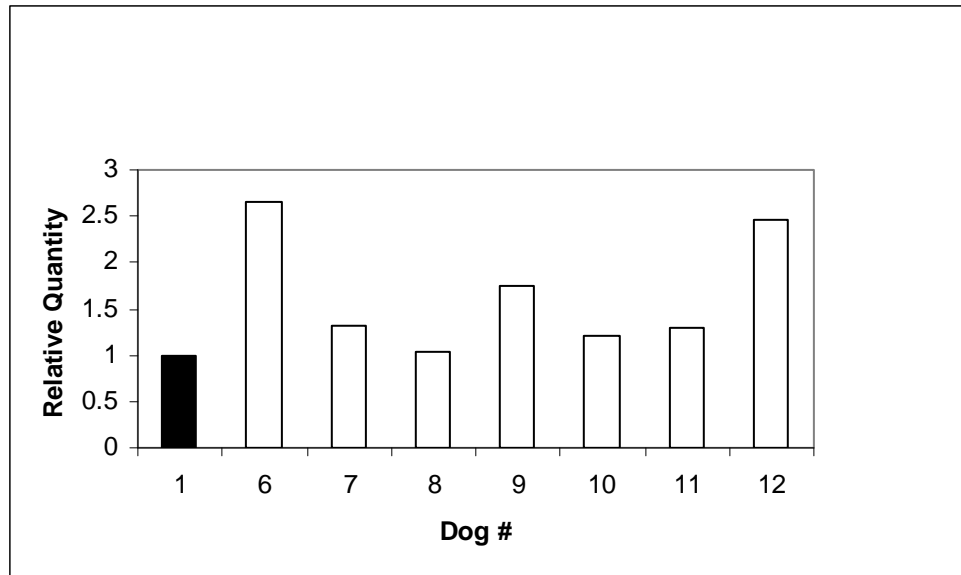


Figure 2.5 Relative amount of leukocyte mtDNA from affected English Springer Spaniel dogs (white bars) calibrated to normal Dog 1 (black bar). The results are expressed as a ratio relative to the value for Dog 1.

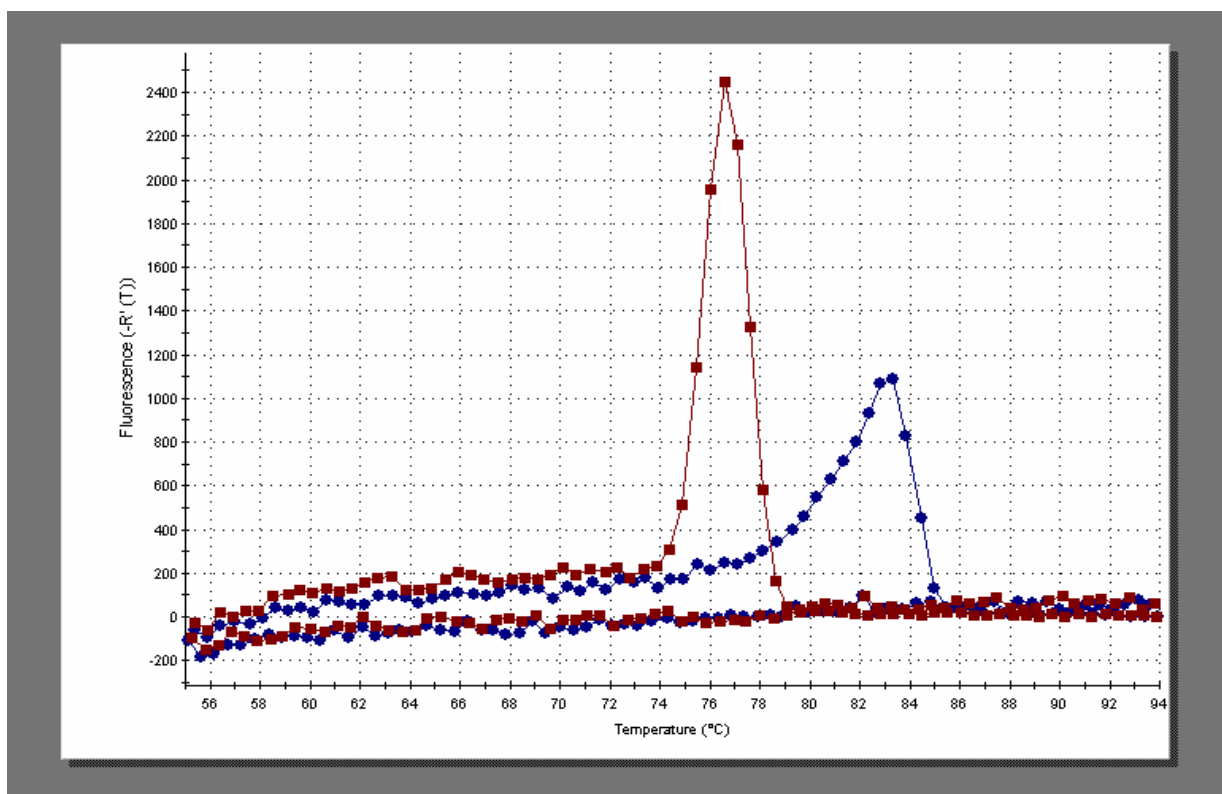


Figure 2.6 Dissociation analysis of real-time COX-1 (■) and GA-3-PDH (●) amplicons. The negative derivative of fluorescence versus temperature was plotted against temperature. The curve shows single peaks, suggesting that only specific PCR products were generated with these sets of primers.

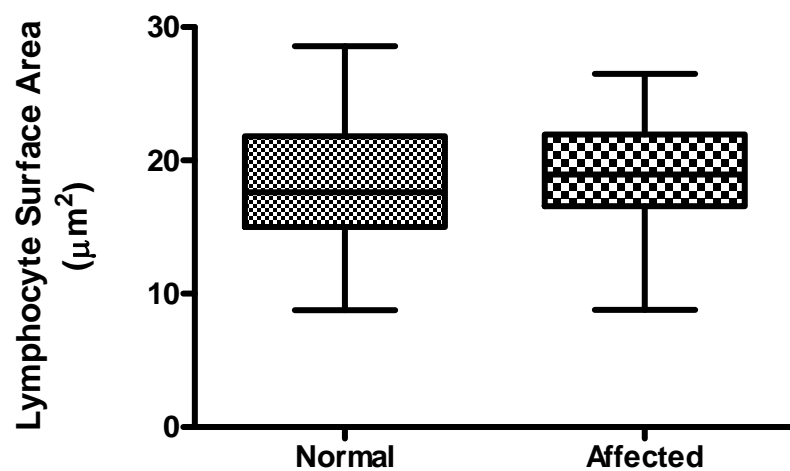


Figure 2.7 Box and whisker graphs of lymphocyte surface area of normal and affected English Springer Spaniel dogs.

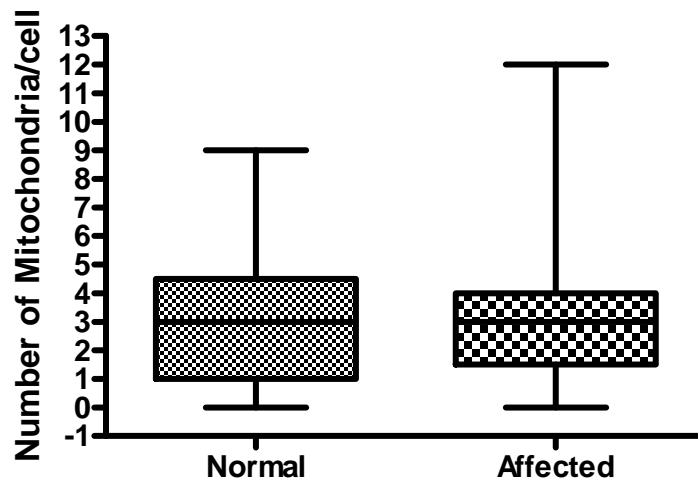


Figure 2.8 Box and whisker graphs of mitochondrial numbers per lymphocyte cross-section of normal and affected English Springer Spaniel dogs.

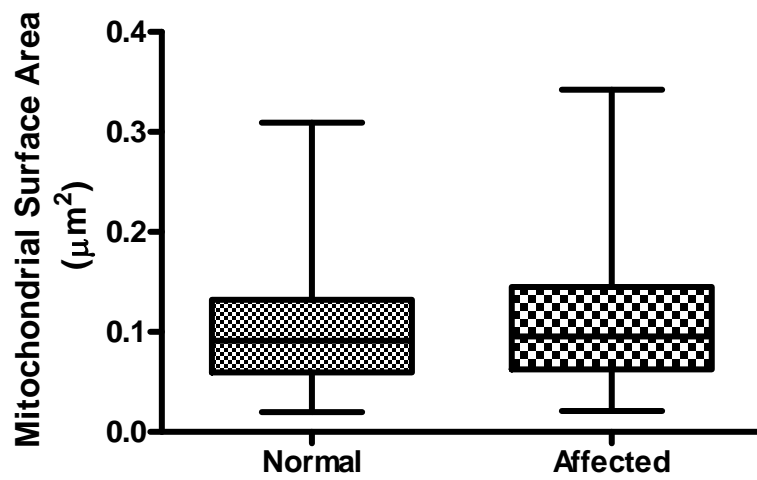


Figure 2.9 Box and whisker graphs of mitochondrial surface area per lymphocyte cross-section of normal and affected English Springer Spaniel dogs.

GENERAL CONCLUSION

This study was undertaken to better understand the roles of TFAM, mitochondria and mtDNA in the pathogenesis of retinal dysplasia in the Miniature Schnauzer and English Springer Spaniel dog. In the Miniature Schnauzer dog the *Tfam* promoter region, intron1, coding and 3'non-coding sequence were amplified and sequenced in normal and affected dogs with no sequence differences between the two groups. The mitochondrial numbers and surface area per lymphocyte cross-sectional area also revealed no differences between affected and normal Miniature Schnauzer dogs. Similarly, lymphocyte mitochondrial morphology could not distinguish healthy dogs from those with retinal dysplasia. With respect to the English Springer Spaniel dog, using real-time PCR it was demonstrated that the relative quantities of leukocyte mtDNA varies widely between affected and unaffected dogs. Similar to the Miniature Schnauzer dog, electron microscopy failed to demonstrate lymphocyte mitochondrial differences between affected and normal dogs.

The original study by Appleyard *et al.*⁴³ demonstrated differential gene expression of mtDNA and *Tfam* in the retina and RPE of an affected Miniature Schnauzer dog, as well as possible morphological changes in the mitochondria of various tissues.⁴³ Based on this study, it was hypothesized that a decreased energy supply to the retina and RPE may lead to retinal dysplasia. The initial representational difference analysis (RDA) performed by Appleyard *et al.*⁴³ provides evidence of decreased mitochondrial DNA or decreased mitochondrial transcription activity in affected Miniature Schnauzer RPE. The RDA technique itself has been demonstrated to be useful for large scale profiling of differential gene expression¹³⁹ and sensitive in identifying rare transcripts with minimal chance of isolating false positive clones.¹⁴⁰ The RDA results of differential mitochondrial gene expression reported by Appleyard *et al.*⁴³ may be valid; however, these observations were followed by real-time PCR using only one affected and one normal dog. Therefore, of significant importance is that the real-time PCR results provided by Appleyard *et al.*⁴³ lack power due to the low sample number used. Using several affected and normal dogs, the data obtained in this particular study does not support the real-time PCR and electron microscopic findings by Appleyard *et al.*⁴³

Identifying differences in retinal or RPE gene expression between affected and normal dogs is an important step towards understanding the pathophysiology of retinal dysplasia. With any technique used to identify differentially expressed genes however, causative genes can be missed. This could occur if expression of these genes occurs only at certain points in development, if technical problems occur with the procedure, or if possible loss of transcripts in the RNA isolation or amplification process occurs. In order to verify the findings by Appleyard *et al.*⁴³ a repeat breeding of affected and confirmed normal dogs to increase sample numbers and obtain retinal and RPE tissue would be necessary. Using the increased sample numbers, nuclear and mitochondrial gene expression differences within the retina and RPE could be evaluated. As retinal dysplasia is a congenital condition¹ and mRNA expression may be influenced by multiple factors including stage of development¹²⁷, determining which genes are differentially expressed by the retina and RPE during the development of retinal dysplasia in utero would be ideal. To determine if mitochondria play a role in the pathogenesis of retinal dysplasia in the Miniature Schnauzer and English Springer Spaniel dog evaluation of mitochondria, mtDNA and mitochondrial gene expression within age-matched retina and RPE would be necessary.

A DNA microarray is an experimental tool that allows for gene expression analysis.¹²⁸ Using this technique, thousands of discrete DNA sequences (arrays) are hybridized to fluorescently labeled DNA or RNA samples and the relative abundance of each gene sequence can be compared by the ratio of fluorescence.¹²⁸ Microarray technology has demonstrated low false positive rates¹⁴¹ but it does however, have its limitations. It cannot be used for gene discovery, as it relies on prefabricated probes to allow for analysis and it has also been known to be problematic to detect changes in transcript profiles for low abundance transcripts because of detector sensitivity limits.¹³⁹ A great deal of information can be obtained through cDNA subtraction methods coupled with microarray screening. Using this strategy, differentially expressed genes are first enriched by RDA, followed by cloning, amplification and then microarray analysis to screen the subtracted products.^{142, 143}

Confirmation of the data obtained by Appleyard *et al.*⁴³ or identification of other candidate genes causing retinal dysplasia could thus potentially be achieved by microarray

gene expression analysis. If mitochondrial genes are isolated by microarray analysis, determining the retinal and RPE mitochondrial content and possibly function during the genesis of retinal dysplasia would also be advantageous. Such further investigations should prove to yield new insights into the pathogenesis of retinal dysplasia in the Miniature Schnauzer and English Springer Spaniel dog.

REFERENCES

1. Whiteley HE. Dysplastic canine retinal morphogenesis. *Invest Ophth Vis Sci*. 1991;32:1492-1498.
2. Rubin LF. Hereditary Retinal Detachment in Bedlington Terriers. A Preliminary Report. *Small Anim Clin*. 1963;3:387-389.
3. Rubin LF. Heredity of retinal dysplasia in Bedlington Terriers. *J Am Vet Med Assoc*. 1968;152:260-262.
4. Crispin SM, Long SE, Wheeler CA. Incidence and ocular manifestations of multifocal retinal dysplasia in the golden retriever in the UK. *Vet Rec*. 1999;145:669-672.
5. Lavach JD, Murphy JM, Severin GA. Retinal dysplasia in the English springer spaniel. *J Am Anim Hosp Assoc*. 1978;14:192-199.
6. Venter IJ, van der Lugt JJ, vanRensburg IBJ, Petrick SW. Multiple Congenital Eye Anomalies in Bloodhound Puppies. *Vet Comp Ophthalmol*. 1996;6:9-13.
7. Ashton N, Barnett KC, Sachs DD. Retinal dysplasia in the Sealyham terrier. *J Pathol Bacteriol*. 1968;96:269-272.
8. Heywood R, Wells GAH. A retinal dysplasia in the Beagle dog. *Vet Rec*. 1970;87:178-180.
9. MacMillan AD, Lipton DE. Heritability of multifocal retinal dysplasia in American Cocker Spaniels. *J Am Vet Med Assoc*. 1978;172:568-572.
10. Bedford PG. Multifocal retinal dysplasia in the rottweiler. *Vet Rec*. 1982;111:304-305.
11. Peiffer RL, Jr., Fischer CA. Microphthalmia, retinal dysplasia, and anterior segment dysgenesis in a litter of Doberman Pinschers. *J Am Vet Med Assoc*. 1983;183:875-878.
12. Laratta LJ, Riis RC, Kern TJ, Koch SA. Multiple congenital ocular defects in the Akita dog. *Cornell Vet*. 1985;75:381-392.
13. Barnett KC, Bjorck GR, Kock E. Hereditary retinal dysplasia in the Labrador Retriever in England and Sweden. *J Small Anim Pract*. 1970;10:755-759.
14. Stades FC. Hereditary retinal dysplasia (RD) in a family of Yorkshire terriers. *Tijdschr Diergeneesk*. 1978;103:1087-1090.
15. Grahn BH, Storey ES, McMillan C. Inherited retinal dysplasia and persistent hyperplastic primary vitreous in Miniature Schnauzer dogs. *Vet Ophthalmol*. 2004;7:151-158.
16. Saroglu M, Devecioglu Y, Altunatmaz K. Fundoscopic normal variations of the retina in Turkish sheepdogs and multifocal retinal dysplasia: a comparative study in Akbash and Kangal breeds. *Turk Veterinerlik ve Hayvancilik Dergisi*. 2005;29:551-556.
17. Martin CL, Leipold HW. Aphakia and multiple ocular defects in Saint Bernard puppies. *Vet Med Sm Anim Clin*. 1974;69:448-453.
18. American College of Veterinary Ophthalmologists Genetics Committee. *Ocular Disorders Presumed to be Inherited in Purebred Dogs*: American College of Veterinary Ophthalmologists 2006:18-19.
19. Narfstrom K, Petersen-Jones, S. Diseases of the Canine Ocular Fundus. In: Gelatt KN (ed), *Vet Ophthalmol*. Iowa: Blackwell Publishing; 2007:944-1025.

20. O'Toole D, Young S, Severin GA, Neumann S. Retinal dysplasia of English springer spaniel dogs: light microscopy of the postnatal lesions. *Vet Pathol.* 1983;20:298-311.
21. Blair NP, Tso, M.O.M, Schmidt, G.M. Vitreoretinal degeneration: An experimental model in Labrador retrievers. *Invest Ophth Vis Sci (Suppl).* 1981;20:122.
22. O'Toole D, Young S. Dysplastic retinal morphogenesis in the English springer spaniel dog. *Proc Amer Soc Vet Oph Int Soc Vet Ophth.* 1982;166-172.
23. Holle DM, Stankovics ME, Sarna CS, Aguirre GD. The geographic form of retinal dysplasia in dogs is not always a congenital abnormality. *Vet Ophthalmol.* 1999;2:61-66.
24. Schmidt GM, Ellersieck MR, Wheeler CA, Blanchard GL, Keller WF. Inheritance of retinal dysplasia in the English Spring Spaniel. *J Am Vet Med Assoc.* 1979;174:1089-1090.
25. Nelson DL, MacMillan AD. Multifocal retinal dysplasia in field trial Labrador Retrievers. *J Am Anim Hosp Assoc.* 1983;19:388-392.
26. Carrig CB, Sponenberg DP, Schmidt GM, Tvedten HW. Inheritance of associated ocular and skeletal dysplasia in Labrador retrievers. *J Am Vet Med Assoc.* 1988;193:1269-1272.
27. Carrig CB, MacMillan A, Brundage S, Pool RR, Morgan JP. Retinal dysplasia associated with skeletal abnormalities in Labrador Retrievers. *J Am Vet Med Assoc.* 1977;170:49-57.
28. Bergsjø T, Arnesen K, Heim P, Nes N. Congenital blindness with ocular developmental anomalies, including retinal dysplasia, in Doberman Pinscher dogs. *J Am Vet Med Assoc.* 1984;184:1383-1386.
29. Arnbjerg J, Jensen, O.A. Spontaneous microphthalmia in two doberman puppies with anterior chamber cleavage syndrome. *J Am Anim Hosp Assoc.* 1982;18:481-484.
30. Lewis D, Kelly DF, Sansom J. Congenital microphthalmia and other developmental ocular anomalies in the Dobermann. *J Small Anim Pract.* 1986;27:559-566.
31. Meyers VN, Jezyk PF, Aguirre GD, Patterson DF. Short-limbed dwarfism and ocular defects in the Samoyed dog. *J Am Vet Med Assoc.* 1983;183:975-979.
32. Lahav M, Albert DM, Wyand S. Clinical and histopathologic classification of retinal dysplasia. *Am J Ophthalmol.* 1973;75:648-667.
33. Grahn BH, Peiffer, R.L. Fundamentals of Veterinary Ophthalmic Pathology. In: Gelatt KN (ed), *Vet Ophthalmol.* Iowa: Blackwell Publishing; 2007.
34. Cook CS. Ocular Embryology and Congenital Malformations. In: Gelatt KN (ed), *Vet Ophthalmol.* Iowa: Blackwell Publishing; 2007:3-36.
35. Albert DM, Lahav M, Carmichael LE, Percy DH. Canine herpes-induced retinal dysplasia and associated ocular anomalies. *Invest Ophth.* 1976;15:267-278.
36. Shively JN, Phemister RD, Epling GP, Jensen R. Pathogenesis of radiation-induced retinal dysplasia. *Invest Ophth.* 1970;9:888-900.
37. Long SE, Crispin SM. Inheritance of multifocal retinal dysplasia in the golden retriever in the UK. *Vet Rec.* 1999;145:702-704.
38. Silverstein A, Osburn BI, Prendergast, RA. The pathogenesis of retinal dysplasia. *Am J Ophthalmol.* 1971;72:13-21.

39. Percy DH, Danylchuk KD. Experimental retinal dysplasia due to cytosine arabinoside. *Invest Ophth Vis Sci.* 1977;16:353-364.
40. Bendixen HC. Littery occurrence of anophthalmia or microphthalmia together with other malformations in swine-presumably due to vitamin A deficiency of the maternal diet in the first stage of pregnancy and the preceding period. *Acta Patho Mic Sc.* 1944;161-179 pp.
41. Millemann Y, Benoit-Valiergue H, Bonnin JP, Fontaine JJ, Maillard R. Ocular and cardiac malformations associated with maternal hypovitaminosis A in cattle. *Vet Rec.* 2007;160:441-443.
42. Gottschall-Pass KT, Grahn BH, Gorecki DK, Paterson PG. Oscillatory potentials and light microscopic changes demonstrate an interaction between zinc and taurine in the developing rat retina. *J Nutr.* 1997;127:1206-1213.
43. Appleyard GD, Forsyth GW, Kiehlbauch LM, et al. Differential mitochondrial DNA and gene expression in inherited retinal dysplasia in Miniature Schnauzer dogs. *Invest Ophth Vis Sci.* 2006;47:1810-1816.
44. Larsson NG, Wang J, Wilhelmsson H, et al. Mitochondrial transcription factor A is necessary for mtDNA maintenance and embryogenesis in mice. *Nat Genet.* 1998;18:231-236.
45. Mitchell PJ, Tjian R. Transcriptional regulation in mammalian cells by sequence-specific DNA binding proteins. *Science.* 1989;245:371-378.
46. Stryer L. *Biochemistry.* 4 ed. New York: W.H. Freeman and Company; 1995.
47. Bornstein P, McKay J, Morishima JK, Devarayalu S, Gelinas RE. Regulatory elements in the first intron contribute to transcriptional control of the human alpha 1(I) collagen gene. *Proc Natl Acad Sci U S A.* 1987;84:8869-8873.
48. Bornstein P, McKay J, Liska DJ, Apone S, Devarayalu S. Interactions between the promoter and first intron are involved in transcriptional control of alpha 1(I) collagen gene expression. *Mol Cell Biol.* 1988;8:4851-4857.
49. Alder H, Yoshinouchi M, Prystowsky MB, Appasamy P, Baserga R. A conserved region in intron 1 negatively regulates the expression of the PCNA gene. *Nucleic Acids Res.* 1992;20:1769-1775.
50. Tee MK, Babalola GO, Aza-Blanc P, Speek M, Gitelman SE, Miller WL. A promoter within intron 35 of the human C4A gene initiates abundant adrenal-specific transcription of a 1 kb RNA: location of a cryptic CYP21 promoter element? *Hum Mol Genet.* 1995;4:2109-2116.
51. Humphrey T, Proudfoot NJ. A beginning to the biochemistry of polyadenylation. *Trends Genet.* 1988;4:243-245.
52. Bernstein P, Peltz, S.W., Ross, J. The Poly(A)-Poly(A)-Binding Protein Complex Is a Major Determinant of mRNA stability in Vitro. *Mol Cell Biol.* 1989;9:659-670.
53. Higgs DR, Goodbourn SE, Lamb J, Clegg JB, Weatherall DJ, Proudfoot NJ. Alpha-thalassaemia caused by a polyadenylation signal mutation. *Nature.* 1983;306:398-400.
54. Whitelaw E, Proudfoot N. Alpha-thalassaemia caused by a poly(A) site mutation reveals that transcriptional termination is linked to 3' end processing in the human alpha 2 globin gene. *Embo J.* 1986;5:2915-2922.
55. Hatefi Y. The mitochondrial electron transport and oxidative phosphorylation system. *Annu Rev Biochem.* 1985;54:1015-1069.

56. Palade GE. An electron microscope study of the mitochondrial structure. *J Histochem Cytochem.* 1953;1:188-211.
57. Taanman JW. The mitochondrial genome: structure, transcription, translation and replication. *Biochim Biophys Acta.* 1999;1410:103-123.
58. Clayton DA. Replication of animal mitochondrial DNA. *Cell.* 1982;28:693-705.
59. Kanki T, Ohgaki K, Gaspari M, et al. Architectural role of mitochondrial transcription factor A in maintenance of human mitochondrial DNA. *Mol Cell Biol.* 2004;24:9823-9834.
60. Shadel GS, Clayton DA. Mitochondrial DNA maintenance in vertebrates. *Annu Rev Biochem.* 1997;66:409-435.
61. Robin ED, Wong R. Mitochondrial DNA molecules and virtual number of mitochondria per cell in mammalian cells. *J Cell Physiol.* 1988;136:507-513.
62. Lee HC, Yin PH, Lu CY, Chi CW, Wei YH. Increase of mitochondria and mitochondrial DNA in response to oxidative stress in human cells. *Biochem J.* 2000;348 (2):425-432.
63. Kim KS, Lee SE, Jeong HW, Ha JH. The complete nucleotide sequence of the domestic dog (*Canis familiaris*) mitochondrial genome. *Mol Phylogenet Evol.* 1998;10:210-220.
64. Poyton RO, McEwen, J.E. Crosstalk between nuclear and mitochondrial genomes. *Annu Rev Biochem.* 1996;65:563-607.
65. Larsson NG, Oldfors A, Holme E, Clayton DA. Low levels of mitochondrial transcription factor A in mitochondrial DNA depletion. *Biochem Biophys Res Commun.* 1994;200:1374-1381.
66. Clayton DA. Replication and transcription of vertebrate mitochondrial DNA. *Annu Rev Cell Biol.* 1991;7:453-478.
67. Scarpulla RC. Transcriptional activators and coactivators in the nuclear control of mitochondrial function in mammalian cells. *Gene.* 2002;286:81-89.
68. Williams RS. Mitochondrial gene expression in mammalian striated muscle. Evidence that variation in gene dosage is the major regulatory event. *J Biol Chem.* 1986;261:12390-12394.
69. Luciakova K, Li R, Nelson BD. Differential regulation of the transcript levels of some nuclear-encoded and mitochondrial-encoded respiratory-chain components in response to growth activation. *Eur J Biochem.* 1992;207:253-257.
70. Parisi MA, Clayton DA. Similarity of human mitochondrial transcription factor 1 to high mobility group proteins. *Science.* 1991;252:965-969.
71. National Center for Biotechnology Information <http://www.ncbi.nlm.nih.gov>; 2008.
72. Dairaghi DJ, Shadel GS, Clayton DA. Addition of a 29 residue carboxyl-terminal tail converts a simple HMG box-containing protein into a transcriptional activator. *J Mol Biol.* 1995;249:11-28.
73. Clayton DA. Transcription and replication of animal mitochondrial DNAs. *Int Rev Cytol.* 1992;141:217-232.
74. Kang D, Kim SH, Hamasaki N. Mitochondrial transcription factor A (TFAM): roles in maintenance of mtDNA and cellular functions. *Mitochondrion.* 2007;7:39-44.

75. Fisher RP, Lisowsky T, Parisi MA, Clayton DA. DNA wrapping and bending by a mitochondrial high mobility group-like transcriptional activator protein. *J Biol Chem.* 1992;267:3358-3367.
76. Alam TI, Kanki T, Muta T, et al. Human mitochondrial DNA is packaged with TFAM. *Nucleic Acids Res.* 2003;31:1640-1645.
77. Falkenberg M, Gaspari M, Rantanen A, Trifunovic A, Larsson NG, Gustafsson CM. Mitochondrial transcription factors B1 and B2 activate transcription of human mtDNA. *Nat Genet.* 2002;31:289-294.
78. Asin-Cayuela J, Gustafsson CM. Mitochondrial transcription and its regulation in mammalian cells. *Trends Biochem Sci.* 2007;32:111-117.
79. Gleyzer N, Vercauteren K, Scarpulla RC. Control of mitochondrial transcription specificity factors (TFB1M and TFB2M) by nuclear respiratory factors (NRF-1 and NRF-2) and PGC-1 family coactivators. *Mol Cell Biol.* 2005;25:1354-1366.
80. Gaspari M, Falkenberg M, Larsson NG, Gustafsson CM. The mitochondrial RNA polymerase contributes critically to promoter specificity in mammalian cells. *Embo J.* 2004;23:4606-4614.
81. McCulloch V, Shadel GS. Human mitochondrial transcription factor B1 interacts with the C-terminal activation region of h-mtTFA and stimulates transcription independently of its RNA methyltransferase activity. *Mol Cell Biol.* 2003;23:5816-5824.
82. Ohgaki K, Kanki T, Fukuoh A, et al. The C-terminal tail of mitochondrial transcription factor a markedly strengthens its general binding to DNA. *J Biochem (Tokyo).* 2007;141:201-211.
83. Ekstrand MI, Falkenberg M, Rantanen A, et al. Mitochondrial transcription factor A regulates mtDNA copy number in mammals. *Hum Mol Genet.* 2004;13:935-944.
84. Matsushima Y, Matsumura K, Ishii S, et al. Functional domains of chicken mitochondrial transcription factor A for the maintenance of mitochondrial DNA copy number in lymphoma cell line DT40. *J Biol Chem.* 2003;278:31149-31158.
85. Li H, Wang J, Wilhelmsson H, et al. Genetic modification of survival in tissue-specific knockout mice with mitochondrial cardiomyopathy. *Proc Natl Acad Sci U S A.* 2000;97:3467-3472.
86. Wang J, Wilhelmsson H, Graff C, et al. Dilated cardiomyopathy and atrioventricular conduction blocks induced by heart-specific inactivation of mitochondrial DNA gene expression. *Nat Genet.* 1999;21:133-137.
87. Ikeuchi M, Matsusaka H, Kang D, et al. Overexpression of mitochondrial transcription factor a ameliorates mitochondrial deficiencies and cardiac failure after myocardial infarction. *Circulation.* 2005;112:683-690.
88. Sambrook J, Russell, D.W. *Molecular Cloning: A Laboratory Manual.* Third ed. Cold Spring Harbor, New York: Cold Spring Harbor Laboratory Press; 2001.
89. Valasek MA, Repa JJ. The power of real-time PCR. *Adv Physiol Educ.* 2005;29:151-159.
90. Taylor GR. Polymerase chain reaction: basic principles and automation. In: McPherson MJ, Quirke, P., Taylor, G.R. (ed), *PCR: A Practical Approach.* New York: Oxford University Press; 1992.
91. Nei M, Li WH. Mathematical model for studying genetic variation in terms of restriction endonucleases. *Proc Natl Acad Sci U S A.* 1979;76:5269-5273.

92. Bachmann HS, Siffert, W., Frey, U.H. Successful amplification of extremely GC-rich promoter regions using a novel 'slowdown PCR' technique. *Pharmacogenetics*. 2003;13:759-766.
93. West C, Pulley EH, Tuner TM, Schmidt GM and Tso MOM. Pathology of inherited retinal dysplasia in the English springer spaniel: an in utero and neonatal study. *Invest Ophth Vis Sci (Suppl)*. 1982;22:57.
94. Whiteley HE, Young S. The external limiting membrane in developing normal and dysplastic canine retina. *Tissue Cell*. 1986;18:231-239.
95. Whiteley HE, Rash, J.E. and Yound, S. Freeze-fracture studies of canine retinal dysplasia. *Invest Ophth Vis Sci (Suppl)*. 1984;25:17.
96. Grahn BH, Storey ES, Cullen CL. Diagnostic ophthalmology. *Can Vet J*. 2002;43:889-890.
97. West CS PE, Tuner TM, Schmidt GM and Tso MOM. Pathology of inherited retinal dysplasia in the English springer spaniel: an in utero and neonatal study. *Invest Ophthalmol Vis Sci (Suppl)*. 1982;22:57.
98. O'Toole D, Young S. Dysplastic retinal morphogenesis in the English springer spaniel dog. *Proc Am Soc Vet Ophthalmol and Int Soc Vet Ophthalmol*. 1982;166-172.
99. Silverstein AM OB, Prendergast, RA. The pathogenesis of retinal dysplasia. *Am J Ophthalmol*. 1971;72:13-21.
100. Silver J, Sidman, R.L. A mechanism for the guidance and topographic patterning of retinal ganglion cell axons. *J Comp Neurol*. 1980;189:101-111.
101. Whiteley HE, Bergstrom RA, Scott JR. Intramembranous particle distribution and filipin binding in dysplastic canine retina. *Curr Eye Res*. 1991;10:1069-1074.
102. Bustin SA. Absolute quantification of mRNA using real-time reverse transcription polymerase chain reaction assays. *J Mol Endocrinol*. 2000;25:169-193.
103. Bustin SA, Nolan T. Pitfalls of quantitative real-time reverse-transcription polymerase chain reaction. *J Biomol Tech*. 2004;15:155-166.
104. Wong ML, Medrano JF. Real-time PCR for mRNA quantitation. *Biotechniques*. 2005;39:75-85.
105. Livak KJ, Schmittgen TD. Analysis of relative gene expression data using real-time quantitative PCR and the 2(-Delta Delta C(T)) Method. *Methods*. 2001;25:402-408.
106. Pfaffl MW. A new mathematical model for relative quantification in real-time RT-PCR. *Nucleic Acids Res*. 2001;29:e45.
107. Rubin LF. *Inherited Eye Diseases in Purebred Dogs*; 1989.
108. Bachmann HS, Siffert W, Frey UH. Successful amplification of extremely GC-rich promoter regions using a novel 'slowdown PCR' technique. *Pharmacogenetics*. 2003;13:759-766.
109. Virbasius JV, Scarpulla RC. Activation of the human mitochondrial transcription factor A gene by nuclear respiratory factors: a potential regulatory link between nuclear and mitochondrial gene expression in organelle biogenesis. *Proc Natl Acad Sci U S A*. 1994;91:1309-1313.
110. Zaid A, Li, R., Luciakova, K., Barath, P., Nery, S., Nelson, B.D. On the role of the general transcription factor Sp1 in the activation and repression of diverse mammalian oxidative phosphorylation genes. *J Bioenerg Biomembr*. 1999;31:129-135.

111. Gerard M, Krol, A., Carbon, P. Transcription factor hStaf/ZNF143 is required for expression of the human TFAM gene. *Gene*. 2007;401:145-153.
112. Huo L, Scarpulla, R. Mitochondrial DNA instability and peri-implantation lethality associated with targeted disruption of nuclear respiratory factor 1 in mice. *Mol Cell Biol*. 2001;21:644-654.
113. Li F, Wang Y, Zeller KI, et al. Myc stimulates nuclearly encoded mitochondrial genes and mitochondrial biogenesis. *Mol Cell Biol*. 2005;25:6225-6234.
114. Wu Z, Puigserver P, Andersson U, et al. Mechanisms controlling mitochondrial biogenesis and respiration through the thermogenic coactivator PGC-1. *Cell*. 1999;98:115-124.
115. Choi YS, Kim, S., Lee, H.K., Lee, K., Pak, Y.K. In vitro methylation of nuclear respiratory factor-1 binding site suppresses the promoter activity of mitochondrial transcription factor A. *Biochem Bioph Res Co*. 2004;314:118-122.
116. Laimins L, Holmgren-Koenig, Monika, Khoury, George. Transcriptional "silencer" elements in rat repetitive sequences associated with the rat insulin 1 gene locus. *Proc Natl Acad Sci U S A*. 1985;83:3151-3155.
117. Day DA, Tuite, M.F. . Post-transcriptional gene regulatory mechanisms in eukaryotes: an overview. *J Mol Endocrinol*. 1998;157:361-371.
118. Jackson RJ, Standart N. Do the poly(A) tail and 3' untranslated region control mRNA translation? *Cell*. 1990;62:15-24.
119. Huez G, Bruck, C., Cleuter, Y. Translational stability of native and deadenylated rabbit globin mRNA injected into HeLa cells. *Proc Natl Acad Sci U S A*. 1981;78:908-911.
120. Poulton J, Morten K, Freeman-Emmerson C, et al. Deficiency of the human mitochondrial transcription factor h-mtTFA in infantile mitochondrial myopathy is associated with mtDNA depletion. *Hum Mol Genet*. 1994;3:1763-1769.
121. Lee H, Wei, Y. Mitochondrial biogenesis and mitochondrial DNA maintenance of mammalian cells under oxidative stress. *Int J Biochem Cell B*. 2005;37:822-834.
122. Herzberg NH, Middelkoop, E., Adorf, M., Dekker, H.L., Van Galen, M.J.M., Van den Berg, M., Bolhuis, P.A., Van den Bogert, C. Mitochondria in cultured human muscle cells depleted of mitochondrial DNA. *Eur J Cell Biol*. 1993;61:400-408.
123. Silva JP, Kohler M, Graff C, et al. Impaired insulin secretion and beta-cell loss in tissue-specific knockout mice with mitochondrial diabetes. *Nat Genet*. 2000;26:336-340.
124. Benard G, Faustin B, Passerieux E, et al. Physiological diversity of mitochondrial oxidative phosphorylation. *Am J Physiol Cell Physiol*. 2006;291:1172-1182.
125. Griparic L, van der Blik, A.M. The Many Shapes of Mitochondrial Membranes. *Traffic*. 2001;2:235-244.
126. Manella CA. The relevance of mitochondrial membrane topology to mitochondrial function. *Biochim Biophys Acta*. 2006;1762:140-147.
127. Iida R, Yasuda T, Aoyama M, Tsubota E, Matsuki T, Kishi K. Age-related changes of gene expression in mouse kidney: fluorescence differential display -- PCR analyses. *Mech Ageing Dev*. 2000;113:135-144.
128. Brown PO, Botstein D. Exploring the new world of the genome with DNA microarrays. *Nat Genet*. 1999;21:33-37.

129. Liu CS, Tsai CS, Kuo CL, et al. Oxidative stress-related alteration of the copy number of mitochondrial DNA in human leukocytes. *Free Radic Res.* 2003;37:1307-1317.
130. Liu CS, Kuo CL, Cheng WL, Huang CS, Lee CF, Wei YH. Alteration of the copy number of mitochondrial DNA in leukocytes of patients with hyperlipidemia. *Ann N Y Acad Sci.* 2005;1042:70-75.
131. Barazzoni R, Short, KR., Nair, KS. . Effects of Aging on Mitochondrial DNA Copy Number and Cytochrome *c* Oxidase Gene Expression in Rat Skeletal Muscle, Liver and Heart. *J Biol Chem.* 2000;275:3343-3347.
132. Masuyama M, Iida R, Takatsuka H, Yasuda T, Matsuki T. Quantitative change in mitochondrial DNA content in various mouse tissues during aging. *Biochim Biophys Acta.* 2005;1723:302-308.
133. Lee H, Lu C, Fahn H, Wei Y. Aging- and smoking-associated alteration in the relative content of mitochondrial DNA in human lung. *Fed Euro Biochem Soc.* 1998;441:292-296.
134. Barrientos A, Casademont J, Cardellach F, Estivill X, Urbano-Marquez A, Nunes V. Reduced steady-state levels of mitochondrial RNA and increased mitochondrial DNA amount in human brain with aging. *Brain Res Mol Brain Res.* 1997;52:284-289.
135. Barrientos A, Casademont J, Cardellach F, et al. Qualitative and quantitative changes in skeletal muscle mtDNA and expression of mitochondrial-encoded genes in the human aging process. *Biochem Mol Med.* 1997;62:165-171.
136. Welle S, Bhatt K, Shah B, Needler N, Delehanty JM, Thornton CA. Reduced amount of mitochondrial DNA in aged human muscle. *J Appl Physiol.* 2003;94:1479-1484.
137. Pesce V, Cormio A, Fracasso F, et al. Age-related mitochondrial genotypic and phenotypic alterations in human skeletal muscle. *Free Radic Biol Med.* 2001;30:1223-1233.
138. Herzberg NH, Middelkoop E, Adorf M, et al. Mitochondria in cultured human muscle cells depleted of mitochondrial DNA. *Eur J Cell Biol.* 1993;61:400-408.
139. Andersson T, Borang S, Unneberg P, et al. Shotgun sequencing and microarray analysis of RDA transcripts. *Gene.* 2003;310:39-47.
140. Wada J, Kumar A, Ota K, Wallner EI, Batlle DC, Kanwar YS. Representational difference analysis of cDNA of genes expressed in embryonic kidney. *Kidney Int.* 1997;51:1629-1638.
141. Troyanskaya OG, Garber ME, Brown PO, Botstein D, Altman RB. Nonparametric methods for identifying differentially expressed genes in microarray data. *Bioinformatics.* 2002;18:1454-1461.
142. Kornblum H, Geschwind D. The use of representational difference analysis and cDNA microarrays in neural repair research. *Restor Neurol Neurosci.* 2001;18:89-94.
143. Welford SM, Gregg J, Chen E, et al. Detection of differentially expressed genes in primary tumor tissues using representational differences analysis coupled to microarray hybridization. *Nucleic Acids Res.* 1998;26:3059-3065.